Polymeric micro-cantilever sensors for biomedical applications

Inauguraldissertation

zur

Erlangung der Würde eines Doktors der Philosophie

vorgelegt der

Medizinischen Fakultät

der Universität Basel

von

Prabitha Urwyler

aus Aarwangen, Kanton Bern, Schweiz

Basel, 2013

Genehmigt von der Medizinischen Fakultät

auf Antrag von

Prof. Dr. Bert Müller (Faklutätsverantwortlichter, Dissertationsleiter)

Prof. Dr.-Ing. Jens Gobrecht (Korreferent)

Dr. med. Till Saxer (Externer Experte)

Prof. Dr. med. Dr. med. dent. Dr. h. c. Hans-Florian Zeilhofer

(Prüfungsvorsitzender)

Basel, den 30. Januar 2012

Prof. Dr. med. Christoph Beglinger
Dekan

ABSTRACT

The invention of atomic force microscopy spurred the development of micro-cantilever-based sensors. Their applications in biomedicine require disposable, low-cost cantilevers for single usage. Polymeric micro-cantilever arrays might be a beneficial alternative to the established silicon-based microstructures which tags a price of about 100 USD per array. The thesis demonstrates that injection-molded polymeric micro-cantilever arrays have characteristics, which compare reasonably well to silicon ones and permit the quantification of medically relevant species. In a first step, cantilevers with micrometer dimensions and aspect ratios as large as 10 were successfully injection molded from polymers including polypropylene and polyvinylidenfluoride. In addition, a hybrid mold concept developed through this work, allowed easy modification of the surface topography leading to a wide range of surface patterned micro-cantilevers. The fabricated micro-cantilevers are gold-coated for optical readout and ease of functionalization. Prior to functionalization, the micro-cantilevers are surface cleaned using ultraviolet-ozone treatment. The effects of the surface cleaning process on the mechanical and chemical stability were systematically studied by varying the exposure time. A process time of 20 min was found suitable as a trade-off between cleaning and stability.

In a second step, the injection molded micro-cantilevers were characterized for their mechanical and morphological properties. Their performance was similar to the established silicon cantilevers with Q-factors in the range of 10-20. Nanoindentation techniques were used to evaluate the elastic modulus of the micro-cantilevers. Synchrotron radiation-based scanning small- and wide-angle X-ray scattering (SAXS, WAXS) techniques were used to quantify crystallinity and anisotropy in polymer micro-cantilevers with micrometer resolution in real space. SAXS measurements confirmed the lamellar nature of the injection-molded semi-crystalline micro-cantilevers showing the expected strong degree of anisotropy along the injection direction. The homogenous cantilever material exhibits a lamellar periodicity increasing with mold temperature but not with injection speed.

In a last step, we demonstrate that polypropylene cantilevers can be used as biosensors for medical purposes in the same manner as the established silicon ones to detect single-stranded DNA sequences and metal ions in real-time. A differential signal of 7 nm was detected for the hybridization of 1 μM complementary DNA sequences. For 100 nM copper ions the differential signal was found to be (36 $\pm$ 5) nm. Nano-mechanical sensing of medically relevant, nanometer-size species is essential for fast and efficient diagnosis.

The developed low-cost micro-cantilever arrays adapted to the geometric requirements of the Cantisens platform will significantly widen the spectrum of applications. Rather simple further adaptations to the fabrication process will allow an easy tailoring for their application in other systems. It may result in dedicated bedside systems for the benefit of patients.

Contents

Acknowledgements

A number of people have contributed to the work presented in this thesis, both scientifically and technically, and by making these years an unforgettable time. It is my pleasure to thank them at this point.

First of all, I am truly thankful to my supervisor, Prof. Bert Mueller, who gave me the opportunity to work on an exceptionally interdisciplinary topic. His patience, guidance and continuous support has been invaluable.

My deep gratitude goes to Prof. Jens Gobrecht, for introducing me into the world of micro and nano, giving me the opportunity to work in the stimulating framework of the INKA-institute, both at LMN-PSI and FHNW, and for being the co-referee of my thesis.

I extend my thanks to Dr. med Till Saxer, for serving on my committee as an external expert.

I am especially indebted to my group leader Helmut Schift, who with his patience, persistence and knowledge gave me support and guidance throughout the realization of this work.

Special thanks go to my DICANS colleague Jasmin Althaus for her generous help, interesting discussions and great collaboration.

My sincere gratitude goes out to Oskar Häfeli (IKT, FHNW, Windisch) for his help, good advice and patience with my injection molding skills. I appreciate his humour and untiring efforts to help me with the cantilever fabrication. Particular thanks goes to Konstantnis Jefimovs (EMPA, Dübendorf) for, very elegantly, fabricating the molds needed in the course of this work, Alfons Pascual (IKT, FHNW, Windisch) and Jochen Köser (ICB, FHNW, Muttenz) for the many interesting discussions and invaluable experimental assistance.

Further, I would like to express my gratitude to Oliver Bunk (Swiss Light Source, PSI, Villigen) and Hans Deyhle (BMC, UniBasel) for introducing me to the wonders of small-angle X-ray scattering and for their assistance with the X-ray characterization studies. Rudy Ghisleni

(EMPA, Thun) is greatfully acknowledged for his generous help, support and interest in the nanoindentation studies.

My heartfelt thanks to Magnus Kristiansen, Clemens Dransfeld, Erich Kramer, Christian Rytka, Werner Raupach (IKT/INKA, FHNW Windisch) and Uwe Pieles (FHNW, Muttenz) with whom I had the pleasure to discuss and share ideas.

The friendly and supportive atmosphere provided by the past and present members of the LMN, BMC, and IKT-INKA team is greatly appreciated. I extend my gratitude to Mirco Altana, Christian Spreu, Edith Meisel, Celestino Padeste, Konrad Vogelsang, Stefan Stutz, Anja Weber, Rolf Schelldorfer, Eugen Deckardt Thomas Neiger and Eugenie Kirk from LMN at the Paul Scherrer Institut, for their timely help and assistance. Mirco, Your SEM skills will always be remembered. Eugenie, thanks for being a great reader and listener in our great discussions over lunch and travel. The last phase of my PhD at the BMC would have been difficult without the timely coffee-breaks and support from Hans, Georg, Florian, Therese, Maggie and Simone. Maggie, thanks for proof reading the introduction at a very short notice. Special thanks go to the members and friends of the IKT/INKA group. I really enjoyed working with all of you and truly appreciate the good times we had together.

Furthermore, I thank our industrial partner, Concentris, for the interesting collaboration, especially Dr. Felicio Battiston. The financial support from the Swiss Nano Institute is greatly acknowledged.

My friends helped me to keep my routine in balance with the *bhajans*, *bhangra*, *garba*, *dal-chawal*, *gup-chup*. Thanks for being there to light up my spirits. My family was a main factor in making this possible so I would like to thank them all. My parents deserve thanks for all the wonderful things they have given me throughout my life, who conscientiously believed in and encouraged my education. I am especially greatful to my husband, Peter, for his patience, encouragement and for backing my choice to embark on this PhD. His belief in me and his never ending support has often helped me a great deal through the ups and downs during the last 3 years. Mini zwei schätzis, Nikash und Tanush, Merci viel mol! Thanks for showering me with your love, concern, enthusiasm and encouragement.

INTRODUCTION

Biosensors in medical applications remain a hugely untapped market, attracting several players. It is estimated that the global market for biosensors will reach $12 billion by 2015 [1]. Highly sensitive sensors capable of rapid, real-time, *in situ* biological and chemical detection are desired. Existing biological and chemical sensing technologies use different physical or chemical principles and detection methodologies. A biosensor is commonly defined as an analytical device that uses a biological recognition system to detect (macro)molecules. Typically biosensors are comprised of two components: (1) the detector or recognition element, which identifies the stimulus or specific binding, and (2) the transducer, which converts this stimulus to a useful output signal [2]. Depending on the output signal type, biosensors can be classified as optical, electrical and mechanical sensors. The waveguide, surface plasmonic resonance (SPR) techniques are optical sensors, while the quartz crystal microbalance (QCM) and cantilevers are examples of mechanical sensors.

Micro-fabricated cantilevers have been used in atomic force microscopy (AFM) since their invention. Micro-cantilever (μC) beams without tips have proved their applicability as miniaturized, ultrasensitive, and fast-responding sensors for application in chemistry, physics, biochemistry, and medicine [3]. The sensor response is a mechanical bending of a cantilever or a shift in the resonance solely due to adsorption of molecules from the environment. The mechanical bending of the cantilever may arise in response to a surface stress, mass loading, or a change in temperature. Various detection methods, including optical laser based, piezoresistive, piezoelectric, and capacitive, have been introduced to measure the bending of μCs in the range of a few nanometers.

A compelling feature of μC sensors is that they operate in air, vacuum, or liquid environments [4]. In gas, μC sensors can be operated as an artificial nose, whereby the bending pattern of a micro-fabricated array of polymer-coated silicon cantilevers is characteristic of the different vapors from solvents, flavors and beverages [3]. When operated in liquid, μC sensor arrays can be used to detect biochemical processes. Each μC is functionalized with a specific biochemical probe receptor, sensitive for detection of the matching target molecule.

A cantilever can be operated in two different modes: the static mode, where the cantilever deflection is monitored, and the dynamic mode, where cantilever resonance frequency shifts are recorded [5]. In the

static mode it is the surface stress generated when molecules selectively adsorb onto one surface of the cantilever that is measured. Cantilever free-end deflection due to surface stress is often quantified using the Stoney formula [4].

Commercially available silicon μCs are generally fabricated by well-established clean-room processes. The high costs compromise many applications and call for low-cost, disposable sensing elements. Polymer-based μCs are preferred over their silicon-based counterparts because of their properties including surface structuring, biocompatibility, low cost, and processability including rapid prototyping.

Micro-fabrication overview

Successful molding of micro-components depends on both the tooling and the molding process [6]. The techniques used for the realization of tools and mold inserts are lithography processes (UV-LIGA), laser micromachining, micro-grinding, electro-discharge machining (EDM) and micro-electrical-discharge machining (μEDM). Studies report that EDM and μEDM methods do not deliver the required surface finish for cantilever tool inserts [6]. Micro-grinding methods provide better surface quality and sharp corner structures, but are of limited use in the fabrication of small micrometer cavities [6].

Polymer μCs can be prepared in a variety of ways, however the type of polymer often determines the fabrication method [4, 7]. An interesting example is the lithographic patterning of high aspect ratio structures in epoxy (SU-8) by UV-exposure, which has similarities to silicon micromachining [8]. In contrast to this, several thermoplastic molding processes such as hot embossing, injection molding (IM), injection compression molding and thermoforming give rise to micro-parts with high precision and repeatability [9, 10].

Hot embossing

Hot embossing involves pressing a *hard* structured surface against a *soft* polymeric surface at elevated temperature. After sufficient holding and cooling times, the hard surface is removed leaving its impression upon the polymeric substrate. This technique has been used to produce microvalves, microsensors, diffraction gratings, and optical devices [10-12]. It can also be used to pattern thin thermoplastic resists coated onto hard substrates which links molding to lithography (thus called nanoimprint lithography).

Micro injection molding

Micro injection molding (μIM) appears to be one of the most efficient processes for the large-scale production of thermoplastic polymer micro-parts [10]. It is a subset of the injection molding process, where a polymer melt is forced into a cavity, allowed to cool, and removed to produce a part that has the same general shape as the cavity. Micromolding has been used to create a slew of different parts including micro-fluidic devices and micro-pumps for biological applications. Once a mold insert is available, several thousand parts can be molded with modest effort. Micro-patterns on the mold can be replicated into the molded device too, making it possible to integrate different dimensions and topographies into one single tool [13].

Reaction injection molding

Reaction injection molding is similar to injection molding, but instead of one polymer, two components are injected into the closed molding tool [10].

Injection compression molding

Injection compression molding is a combination of IM and embossing to overcome the problem of using the tool to heat the polymer. The melted polymer is injected from a screw into the semi-closed molding tool and then pressed into the micro structures by closing the tool. In this way, the problem of injection through a small gap is avoided when producing a micro structure on a thin carrier layer [10]. A prominent example for injection compression molding is the fabrication of DVD disks with sub-micrometer features.

While the μIM of thermoplastic polymers is the most promising method for the large-scale replication of micro parts [9, 10], hot embossing is most popular on the laboratory scale, because it is more flexible and more delicate structures can be produced [10]. Polystyrene (PS) cantilever beams of thicknesses between 2 to 40 μm with a stiffness ranging from 0.01 to 10 Nm^{-1} have been produced using μIM [14]. Polymer μCs fabricated by fast and cost-effective laser machining processes using polymer films have also been reported [15].

Applications of micro-cantilevers

The first applications of μCs were to map out surface topographies using the scanning tunneling microscopy (STM) and AFM, where the probe tip is dragged (contact mode) over the surface to cause deflection of the μC [16]. For soft surfaces, such as biological cells, tapping mode was developed where the probe tip close to the surface is actuated and the changes in the resonance frequency are monitored.

Applications in the field of biology and chemistry involve the sensing of interactions or conformational changes that occur on one or both sides of the μC. All bio-molecular interactions are in principle detectable using μC technology as long as surface stress is induced due to the specific interaction. In the field of nanomechanical transduction, a promising area is the use of μC arrays for bio-molecular recognition of nucleic acids, proteins and ions [17]. Silicon-based μCs have been used in many sensing studies. In 2000, J. Fritz et al. [18] reported the specific transduction of DNA hybridization and receptor-ligand binding to a direct bending response. In 2001, G. Wu et al. [19] reported 0.2 ng/ml concentration prostate-specific antigen (PSA) detection by silicon nitride μCs with various dimensions. Detection of single vaccinia virus particle with an average mass of 9.5 fg has been also reported. Experiments have shown that the cantilever array technique could also be applied as an artificial nose for analyte vapors [20] along with breath analysis for intensive-care patients [21]. In the field of biotechnology, DNA hybridization between self-complementary strands leads to conformational changes, which result in the bending of a cantilever sensor. Single-stranded DNA (ssDNA) or oligonucleotides are covalently immobilized on a gold-coated cantilever by means of thiol chemistry [18]. When the complementary ssDNAs are exposed to the functionalized cantilever, they hybridize (forming double-stranded DNA) with the ssDNA SAM inducing a surface stress, which is measured as a deflection of the cantilever.

In the field of biomaterials, μCs hold huge potential for studying cell-material interactions. Silicon-based rigid pillars and vertical cantilevers have been used to study cell forces [22, 23]. The essential cell-substrate and cell-cell interactions which are characteristic for *in-vivo* situations are not accounted in the previously used methods. The detection of the contractile forces by means of cantilever bending approach allows measuring forces in the pico-Newton range. Fabrication of polymeric cantilevers with various aspect ratios from a single silicon mold via a micromolding process has been demonstrated for cellular force measurements in isolated cardiac myocytes [24]. Köser et al. [25] reported the successful implementation of the cantilever bending approach using Si-μCs to measure contractile cell forces.

This approach can be well extended and explored using disposable polymer μCs allowing fundamental studies on cell-materials interactions but also realizing cell-based biosensors, which are encouraging for the characterization of implant surfaces. It is an established fact that an implant with rough surfaces both on the micrometer and nanometer scale influences cellular processes such as adhesion, proliferation and differentiation. Chou et al. [26] reported that surface topography alters cell shape and function. Cells on grooved surfaces migrate along the grooves whereby the long axis of the cells is mainly parallel to the grooves [27]. Brunette et al. [28] showed that fibroblasts aligned themselves with the major grooves when concurrently exposed to micromachined major and minor grooves on silicon wafers. Thus tailoring of the cantilever surface morphology on the micrometer scale can significantly increase the bending signal to be detected. Structuring of silicon substrates is a multistep, tedious process whereas tailoring the surface morphology of the polymeric μCs can be easily achieved using the replication methods described earlier. Different dimensions and topographies can be easily incorporated into a single tool using the molding methods making way for a palette of surface patterned polymeric μCs. Surface structuring of polymeric μCs along with the cantilever bending approach appears to be a useful technique in investigating the effect of surface patterns and roughness on cell forces.

Thesis Goals and Contributions

The engineering part of the thesis focuses on the design and fabrication of disposable polymeric μCs with mechanical properties that yield comparable results to the silicon-based ones. The bioscience part concentrates on the functionalization of and molecule adsorption onto the polymeric μCs produced. The target of this research is the demonstration of disposable polymeric μCs as biosensors to quantify and detect molecule adsorption under intentionally modified conditions.

Being interdisciplinary, this thesis demands expertise from several fields, which were provided by numerous groups and persons throughout the various phases of the project. This is a summary of my contribution to this multi-faceted work.

Polymer survey: An initial polymer literature survey was conducted for the plausible polymers to be used for the disposable μCs. The selection criteria of biocompatibility, availability, processability, melt flow rate (MFR), Young's modulus (*E*) and cost narrowed down the selection to a few polymers, namely poly(etheretherketone) (PEEK: Solvay Advanced Polymer AvaSpire AV-650 BG15, Solvay Advanced Polymer KetaSpire KT-880NT, Victrex 150G), poly(propylene) (PP: Moplen SM 6100),

polyoxymethylene copolymers (POM-C: 511P Delrin NC010), cyclic olefin copolymers (COC: Topas 8007X10), polyvinylidenfluoride (PVDF: Kynar 720 Arkema) and liquid crystal polymer (LCP: Vectra A 390).

Injection molding: Cantilevers with micrometer dimensions and aspect ratios as large as 10 were successfully injection molded from polymers including polypropylene (PP) and polyvinylidenfluoride (PVDF). This required replacement of the first generation mold-insert designed for an existing three plate handy-mold with a second generation mold-insert. The design of this second generation mold-insert using CAD software (solidEdge) was equally fun and challenging. The design consisted of 2 arrays, each with different μC cavity depth (35 μm and 45 μm). The feeding channels to the array holder parts and the placement of heat cartridges were re-designed considering inputs from the mold-flow simulation experts. With great technical support from O. Häfeli, the handling of the injection molding machine went on smoothly. Fine tuning the process parameters for a filling shot was mastered after months of hands-on training.

Steel selection for mold: Iterative trials of steel hardening, surface polishing and laser ablation lead to selection of the high quality, fine grained mold-material (Polmax; Uddeholm) for all future molds.

Gold coating: Traditional metal *wafer-like* holders of the evaporator (BALZERS BAE250) were upgraded to gold coat a complete batch of injection molded μCs in one single step. A metal coating of 20 nm gold over 4 nm chromium was found to be optimal for sufficient laser beam reflectivity to use the Cantisens® Research system (Concentris GmbH, Basel, Switzerland).

Surface structuring: A hybrid method (basic idea by H. Schift) was developed and realized to fabricate surface patterned μCs. It allowed easy modification of the surface topography leading to a wide range of surface patterned micro-cantilevers, in one single fabrication step. A thin patterned foil prepared by hot embossing was used as an insert in the second generation mold, forming the interface between the two units of the IM machine. Various micro-patterns were transferred via this form of replication. The topographically different μCs were also characterized in a similar fashion to the non-patterned μCs. A patent application was submitted describing the surface patterning of molded parts using this hybrid mold approach.

Concentris device: With a great introduction from J. Köser, the Cantisens® Research system was explored completely and handled individually across a range of tests (heat tests, chemisorption of thiols, ion

sensing, DNA hybridization). Bending of the different polymeric μCs was quantified using the static cartridge performing heat tests both in air and water. The resonance frequencies both in air and water were experimentally determined using the Cantisens® Research system's dynamic cartridge. The Q-factors were estimated directly from the frequency spectra. Bending due to the surface-stress was recorded during the chemisorption of thiols on the gold coated μCs.

Nanoindenter: A kind gesture from R. Ghisleni (EMPA Thun) gave me an opportunity to learn about and operate the MTS XP nanoindenter. The stiffness of the μCs was determined by nanoindentation using a nanoindenter (MTS XP®, Berkovich tip XPT-12761-0). Bending tests were also performed to qualitatively differentiate the surface patterned cantilevers.

Ultraviolet ozone cleaning: Prior to functionalization, the micro-cantilevers were surface cleaned using a commercially available ultraviolet-ozone (UVO) device. For studying the sensitivity and degradation potential of the UVO treatment, batches of μCs were exposed to UVO for the stipulated time. Bending and nanoindentation tests were conducted using the MTS XP nanoindenter to study the deformation behavior. Behavior during heat tests, bending and indentation was also characterized. The differential scanning calorimeter (DSC) analysis and reflection Fourier transmission infrared (FT-IR) figures were provided by A. Pascual. A process time of 20 min was found to give a suitable trade-off between cleaning and stability.

Structural characterization: Spatially resolved small angle X-ray scattering (SAXS) and wide angle X-ray scattering (WAXS) measurements for the structural characterization was conducted at the cSAXS beamline (Swiss Light Source, Paul Scherrer Institut, Switzerland). Being not so familiar with this type of analysis, it took more effort to achieve to the project goals. Data analysis (using scripts provided by beamline scientists) and figures were prepared for the manuscript. H. Deyhle provided the degree of orientation and the azimuthal plots.

Variotherm injection molding: To increase sensitivity and signal response of the micro-cantilevers, 25 μm thin-cantilevers were fabricated using a third generation mold (designed by T. Iten and O. Häfeli) incorporating the variotherm heating system. Software skills were of great help in programming the machine for the right signal and trigger. The variotherm injection molding has been a dream for many teams working in micro-injection molding projects. Static deflection of the variotherm molded micro-cantilevers was characterized with heat cycling tests and self-assembled monolayer (SAM) formation.

Functionalization unit: The 25 μm-thin PP-μCs were functionalized with experiment specific functionalization solution (provided and prepared by J. Köser). Functionalization of the μCs with probe molecules by insertion into an array of dimension-matched disposable glass capillaries filled with functionalization solution was a challenge demanding patience and precision.

Sensing experiments: The 25 μm-thin PP μCs were tested for biosensing. Detection of DNA hybridization of two 60-70% homologous strands was conducted using protocols from Si-sensing experiments. The Copper sensing was achieved using the trapping capability of the tripeptide glutathione. Calcium sensing, cholesterol sensing and SAM layer formation experiments were also performed but could not be reproduced and hence are not reported within this thesis.

Cell force measurements: Protocols for measurement of cell force using the injection molded μCs were developed in collaboration with J. Althaus. Cells (MG63, C2C12, Rat2) were passaged, splitt and seeded on PP and PVDF μCs with introduction from J. Althaus. Limitations of the low-density, floating μCs for cell seeding were overcome using dedicated holders. Cell force measurements using the Concentris device are not reported due to loss of the seeded cells on insertion into the measurement chamber.

This thesis is based on manuscripts associated with the achievement of the thesis goals:

Chapter 2: P. Urwyler, O. Häfeli, H. Schift, J. Gobrecht, F. Battiston, B. Müller, Disposable polymeric micro-cantilever arrays for sensing, Procedia Engineering 5 (2010) 347-350

Chapter 3: P. Urwyler, H. Schift, J. Gobrecht, O. Häfeli, M. Altana, F. Battiston, B. Müller, Surface patterned polymer micro-cantilever arrays for sensing, Sensors and Actuators A 172 (2011) 2-8

Chapter 4: P. Urwyler, A. Pascual, P. M. Kristiansen, J. Gobrecht, B. Müller, H. Schift, Mechanical and chemical stability of injection molded micro-cantilevers for sensing, J. Appl. Polymer Sci. (submitted)

Chapter 5: P. Urwyler, H. Deyhle, O. Bunk, P. M. Kristiansen, B. Müller, Nanometer-size anisotropy of injection molded polymer micro-cantilever arrays, J. Appl. Phys. (submitted)

Chapter 6: P. Urwyler, J. Köser, H. Schift, J. Gobrecht, B. Müller, Nano-mechanical transduction of polymer micro-cantilevers to detect bio-molecular interactions, Biointerphases DOI 10.1007/s13758-011-0006-6 (in press)

Besides the paper mentioned above, the following abstracts have also been published:

P. Urwyler, O. Häfeli, H. Schift, J. Gobrecht, B. Müller, Disposable Polymeric Micro-Cantilever Arrays for Biomedical Applications, European Cells and Materials 20 (2010) 48

P. Urwyler, O. Häfeli, H. Schift, J. Gobrecht, F. Battiston, B. Müller, Polymeric micro-cantilever arrays for sensing, European Cells and Materials 20 (2010) 261

P. Urwyler, J. Köser, H. Schift, J. Gobrecht, F. Battiston, B. Müller, Injection-moulded micro-cantilever arrays for detecting DNA sequences, European Cells and Materials 22 (2011) 29

Chapter 2 details the work on injection molding high aspect ratio polymeric micro-cantilevers and their subsequent mechanical characterization. Chapter 3 describes a novel hybrid mold concept for tailoring the surface topography of the molded cantilevers in a single fabrication step. Chapter 4 presents the study involved in finding a suitable time window for ultraviolet ozone cleaning of cantilever surfaces. Chapter 5 deals with X-ray scattering techniques used to study the lamellar nature of the injection molded semi-crystalline micro-cantilevers and their degree of anisotropy. The variation of the lamellar periodicity with mold temperature is also discussed here. Chapter 6 thoroughly discusses the work to attain the bioscience goal. Variothermally injection molded 25 μm-thin μCs were tested to detect DNA hybridization and metal ions in real time. The dissertation closes with conclusions presented in Chapter 7, along with recommendations for future work.

The acceptance of μC sensors in research and commercial and analytic applications crucially depends on the robustness, ease of use, reproducibility and associated costs. The ability to mold cantilevers which a) perform similarly to established silicon cantilevers, with Q-factors in the range of 10 to 20, and b) can be functionalized without involving modifications of the manufacturing process, shows the favorable prospects of injection molding in comparison to sophisticated but complex silicon manufacturing technology. These approaches will reduce cost, making micro-cantilever based sensing platforms tenable to a larger audience and employ further materials to allow for sensing applications in medicine and beyond.

1. Global Industry Analysts, Biosensors in medical diagnostics: A global strategic business report (2011)

2. A. F. Collings and F. Caruso, Biosensors recent advances, Rep. Prog. Phys. 60 (1997) 1397-1445.

3. H. P. Lang and C. Gerber, Microcantilever sensors, Top Curr. Chem. 285 (2008) 1-27.

4. K. Goeders, J. Colton and L. Bottomley, Microcantilevers: Sensing chemical interactions via mechanical motion, Chem. Rev. 108 (2008) 522-542.

5. E. Finot, A. Passian and T. Thundat, Measurement of mechanical properties of cantilever shaped materials, Sensors 8 (2008) 3497-2541.

6. J. Zhao, K. Ramesh, G. Chen and M. S. Yong, A study on micro tooling and moulding processes of polymer cantilevers for sensor applications, SIMTech Technical Report 1 (2004) 8

7. G. Genolet, M. Despont, P. Vettiger and D. Anselmetti, All-photoplastic, soft cantilever cassette probe for scanning force microscopy, J. Vac. Sci. Technol. B 18 (2000) 617-620.

8. S. K. M. Nordström, S. Keller, M. Lillemose, A. Johansson, S. Dohn, D. Haefliger, G. Blagoi, M. Havsteen-Jakobsen and A. Boisen, SU-8 cantilevers for bio/chemical sensing; fabrication, characterisation and development of novel read-out methods, Sensors 8 (2008) 1595-1612.

9. J. Giboz, T. Copponnex and P. Mélé, Microinjection molding of thermoplastic polymers: a review, J. Micromech. Microeng. 17 (2007) 96–109.

10. M. Heckele and W. K. Schomburg, Review on micro molding of thermoplastic polymers, J. Micromech. Microeng. 14 (2004) R1-R14.

11. K. Knop, Color pictures using the zero diffraction order of phase grating structures, Opt. Commun. 18 (1976) 298-303.

12. C. Goll, W. Bacher, B. Büstgens, D. Maas and W. K. Schomburg, Electrostatically actuated polymer microvalve equipped with a movable membrane electrode, J. Micromech. Microeng. 7 (1997) 224-226.

13. H. Schift, C. David, M. Gabriel, J. Gobrecht, L. Hyderman, W. Kaiser, S. Körpel and L. Scandella, Nanoreplication in polymers using hot embossing and injection molding, Microelectron. Eng. 53 (2000) 171-174.

14. A. W. McFarland, M. A. Poggi, L. A. Bottomley and J. S. Colton, Injection moulding of high aspect ratio micron-scale thickness polymeric microcantilevers, Nanotechnology 15 (2004) 1628-1632.

15. R. Zhang and X. Xu, Development of a biosensor based on laser-fabricated polymer microcantilevers, Appl. Phys. Lett. 85 (2004) 2423-2425.

16. G. Binning, H. Rohrer, C. Gerber and E. Weibel, Surface studies by scanning tunneling microscopy, Phys. Rev. Lett. 49 (1982) 57-61.

17. M. Ghatkeser, H. Lang, C. Gerber, M. Hegner and T. Braun, Comprehensive characterization of molecular interactions based on nanomechanics, PLoS ONE 3 (2008) e3610.

18. J. Fritz, Translating biomolecular recoginition into nanomechanics, Science 288 (2000) 316-318.

19. G. Wu, R. H. Datar, K. M. Hansen, T. Thundat, R. J. Cote and A. Majumdar, Bioassay of prostate-specific antigen (PSA) using microcantilevers, Nature Biotech. 19 (2001) 856-860.

20. M. Baller, H. Lang, J. Fritz, C. Gerber, J. Gimzewski, U. Drechsler, H. Rothuizen, H. Despont, P. Vettiger, F. Battiston, J. Ramseyer, P. Fornaro, E. Meyer and H.-J. Güntherodt, A cantilever array-based artificial nose, Ultramicroscopy 82 (2000) 1-9.

21. D. Schmid, H. Lang, S. Marsch, C. Gerber and P. Hunziker, Diagnosing disease by nanomechanical olfactory sensors Eur. J. Nanomed. 1 (2008) 44-47.

22. C. G. Galbriath and M. P. Sheetz, A micromachined device provides a new bend on fibroblast traction forces, Proc. Natl. Acad. Sci. 94 (1997) 9114-9118.

23. S. Petronis, J. Gold and B. Kasemo, Microfabricated Force-Sensitive Elastic Substrates for Investigation of Mechanical Cell and Substrate Interactions, J. Micromech. Microeng. 13 (2003) 900-913.

24. Y. Zhao and X. Zhang, Adaptation of flexible polymer fabrication to cellular mechanics study, Appl. Phys. Lett. 87 (2005) 144101-144103.

25. J. Köser, S. Gaiser and B. Müller, Contractile cell forces exerted on rigid substrates, Eur. Cells and Mat. 21 (2011) 479-487.

26. L. Chou, J. D. Firth, V.-J. Uitto and D. Brunette, Substratum surface topography alters cell shape and regulates fibronectin mRNA level, mRNA stability and assembly in human fibroblasts, J. Cell Sci. 108 (1995) 1563-1573.

27. J.-P. Kaiser, A. Reinmann and A. Bruinink, The effect of topographic characteristics on cell migration velocity, Biomaterials 27 (2006) 5230-5241.

28. D. M. Brunette, Fibroblasts on micromachined substrata orient hierarchically to grooves of different dimensions, Exp.Cell Res. 164 (1986) 11-26.

Available online at www.sciencedirect.com
ScienceDirect
Procedia Engineering 5 (2010) 347–350
Procedia Engineering
www.elsevier.com/locate/procedia

Proc. Eurosensors XXIV, September 5-8, 2010, Linz, Austria

Disposable Polymeric Micro-Cantilever Arrays for Sensing

Prabitha Urwyler[a,b,*], Oskar Häfeli[c], Helmut Schift[a], Jens Gobrecht[a,c], Felice Battiston[d], Bert Müller[b]

[a]*Paul Scherrer Institut, Laboratory for Micro- and Nanotechnology, CH-5232 Villigen PSI, Switzerland*
[b]*Biomaterials Science Center, University of Basel, c/o University Hospital, CH-4031 Basel, Switzerland*
[c]*University of Applied Sciences Northwestern Switzerland, School of Engineering, CH-5210 Windisch, Switzerland*
[d]*Concentris GmbH, Davidsbodenstrasse 63, CH-4012 Basel, Switzerland*

Abstract

To fabricate low-cost polymeric cantilever arrays, we have applied injection molding. For polymers, including polypropylene and polyvinylidenfluoride, cantilever dimensions in the micrometer range with an aspect ratio as large as 10 were successfully manufactured. The cantilevers show a performance similar to the established silicon cantilevers. Combined with functionalization, the cantilever arrays show a great potential in biomedical applications.

Keywords: Micro-cantilever; polymer; sensor; injection molding

1. Introduction

Micro-Cantilevers (Cs), similar to those used in scanning force microscopes, have become increasingly popular as transducers in chemical and biological sensors. Various detection methods are introduced to measure the bending of the Cs, which is in the range of few nanometers resulting in extremely high sensitivity. A compelling feature of C sensors is that they can operate in air, vacuum, or liquid [1]. In the field of biomedicine, silicon-based Cs are typically applied, but for single use they are often too expensive, due to the need of clean-room based micro-machining processes. Polymer materials offer tailored physical and chemical properties that can be combined with low-cost mass production. Polymeric Cs are preferred over silicon-based, because of their tunable properties including biocompatibility, low-cost and rapid prototyping along with fitting mechanical properties, which make them particularly sensitive. Despite their advantages over silicon-based cantilever arrays, polymeric C arrays are not yet commercially available.

Cantilevers convert forces acting on them into a deflection [2], thereby relying on their deflection to indicate sensing. Forces in the pN-range can be detected which correspond to a sub-nanometer deflection of the apex of the C sensor. The detectable forces comprise expansions or contractions acting on one side of the cantilever surface,

* Corresponding author. Tel.: +41 56 310 2430; fax: +41 56 310 2646.
E-mail address: prabitha.urwyler@psi.ch

1877-7058 © 2010 Published by Elsevier Ltd.
doi:10.1016/j.proeng.2010.09.119

since they cause bending [2]. Both dynamic and static modes are used in sensing applications. In the static mode it is the surface stress generated when molecules selectively adsorb onto one surface of the cantilever that is measured. Cantilever free-end deflection due to surface stress is often quantified using the Stoney formula [1]. The sensitivity of the sensor depends on Young's modulus E and the cantilever thickness. In order to fabricate polymeric Cs with a sensitivity comparable to silicon ones, they should be one order of magnitude thicker to compensate the lower E.

Polymeric Cs can be fabricated in a variety of ways. The type of polymer often determines the fabrication method [1]. Polymeric Cs previously reported were prepared using photolithography, so only a limited number of materials are suitable and their fabrication is rather expensive [3]. Molding of micro-components from thermoplastic polymers has become a routinely used industrial production process and is one of the most promising fabrication techniques for non-electronic micro devices [4]. Fabrication costs of molded micro-parts are hardly affected by the complexity of the design. Once a mold insert is available, several thousand parts can be molded with little effort. The cost of the raw material in most cases is negligibly low, because only small material quantities are required for micrometer-sized components. Therefore, parts fabricated by micro-molding, even from high-end materials, are suitable for applications requiring low-cost and disposable components [4]. Several molding processes such as hot embossing, micro-injection molding (μIM), reaction injection molding, injection compression molding and thermoforming (IM) give rise to thermoplastics micro-parts [5,6]. Polymeric replication techniques based on nano imprinting and polymer casting can be used to produce polymeric nanometer-sized structures with high precision and repeatability. The hot embossing and the μIM seem to be the most industrially viable processes for molded micro-parts [5]. Polystyrene (PS) cantilever beams of thicknesses between 2 to 40 µm with a stiffness ranging from 0.01 to 10 Nm^{-1} were produced using IM [1]. The acceptance of C sensors in research crucially depends on the robustness, the ease of use, the reproducibility and finally the price. The question arises if disposable polymeric micro-cantilever arrays can be fabricated on the basis of standard thermal IM using precisely machined metal molds. It is the aim of the present scientific activity to adapt IM, well established on the millimeter scale and above, to molds with 30 µm-thin cavities, 500 µm long and 100 µm wide to realize polymeric µCs with a performance comparable or even better to the presently used silicon-based arrays.

2. Experimental details

The polymers used are different grades of poly(etheretherketone) (PEEK: Solvay Advanced Polymer AvaSpire AV-650 BG15, Solvay Advanced Polymer KetaSpire KT-880NT, Victrex 150G), poly(propylene) (PP: Moplen SM 6100), polyoxymethylene copolymers (POM-C: 511P Delrin NC010), cyclic olefin copolymers (COC: Topas 8007X10), polyvinylidenfluoride (PVDF: Kynar 720 Arkema) and liquid crystal polymer (LCP: Vectra A 390).

High quality steel (Polmax Uddeholm) mold inserts were fabricated using laser ablation (Fig. 1, left micrograph) and fixed in the three-plate molding tool 'handy mold'. The Arburg 320 Allrounder (ARBURG, Lossburg, Germany) with a maximum clamping force of 600 kN served for injection molding. The tool temperatures were varied up to 160 °C with water heating and to 260 °C with oil heating. Further process parameters are summarized in Table 1. Complete filling of the mold cavities was observed for all polymers (Fig. 2 left micrograph for PP) with the exception of PEEK, which needs higher processing temperatures than 260 °C.

The injection-molded Cs were coated with 20 nm-thin gold films using an evaporator (BALZERS BAE250). This film guarantees sufficient laser beam reflectivity to use the Cantisens® Research system (Concentris GmbH, Basel, Switzerland) for measuring the resonant frequency and the deflection of the C.

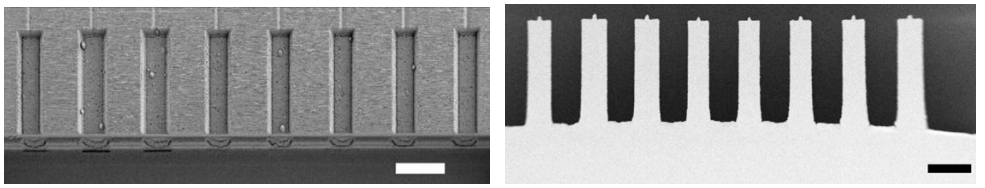

Fig. 1. The left SEM micrograph shows the array of eight laser ablated cantilever cavities in the steel mold insert. The cavity width varies from 80 to 130 µm. The scale bar corresponds to 200 µm. The micrograph on the right is an image of an injection-molded PP micro-cantilever array.

Table 1. Injection molding process parameters for different polymers. The same parameters are valid for all grades of PEEK.

Parameters / Material	COC	PP	PEEK	POM-C	LCP	PVDF
Melting temperature [°C]	240	200	400	220	300	220
Tool temperature [°C]	77	40	225	120	150	120
Tool insert temperature [°C]	-	-	260	-	-	-
Injection speed [cm^3/s]	30	9	10	10	10	10

3. Results and Discussion

With the exception of the high-performance polymer PEEK, which requires mold temperatures of up to 320 °C, the cantilevers reveal the expected thermal behavior as demonstrated in the left diagram of Fig. 2 for the gold-coated PVDF cantilever in air and water. The heat test included a temperature increase from 25 to 35 °C at about t = 0.5 min and a decrease back to 25 °C at about t = 3.2 min. The heat test indicates the sensitivity of the cantilevers that corresponds to deflections of the order of 10 nm. The deflection signal exhibits an exponential, asymptotic behavior. For the temperature difference of 10 K the maximal deflection for PVDF µCs in air corresponds to (95 ± 16) nm and (55 ± 5) nm for thicknesses of 30 µm and 40 µm, respectively. In water, these values increase to (127 ± 17) nm and (154 ± 55) nm as the result of the refraction at the interfaces.

The Cantisens® Research system permits the experimental determination of resonance frequencies f and quality factors Q for the polymeric µCs. Table 2 summarizes the mean values and related standard deviations of the resonance frequency measurements for the Cs in air and water.

The resonance frequency expected is estimated using the µC-length L, the µC-thickness t, the polymer density ρ and the bulk elastic modulus E of the polymer. The deviations of the experimental data from the estimated ones are reasonably explained accounting for dimensional variations as well as the frequency dependence on E. The drop in resonance frequency in water results from the damping, which lowers the Q-factor of the Cs as given in Table 2. The Q-factors were estimated directly from the frequency spectra.

Table 2. Mean values and related standard deviations of the resonance frequency as well as quality factor in air and water.

Polymer	30 µm PP	40 µm PP	30 µm PVDF	40 µm PVDF	30 µm POM-C
Frequency f in air [kHz]	48 ± 3	50 ± 1	60 ± 3	79 ± 5	60 ± 4
Frequency f in water [kHz]	37 ± 8	33 ± 27	43 ± 5	52 ± 5	36 ± 7
$f = 0.162\ t/L^2\ \sqrt{E/\ }$ [kHz]	38	46	66	88	78
Q-factor in air	28	46	38	19	33
Q-factor in water	20	11	10	9	19

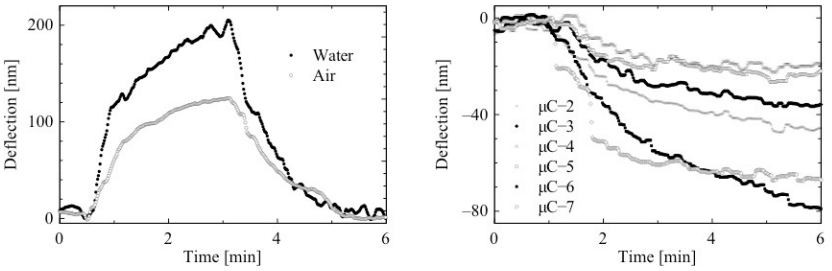

Fig. 2. (a) heat test of 30 µm-thin injection-molded PVDF µCs; (b) deflection curve of 60 µm-thin PVDF µCs during the binding with thiol molecules on the gold-coated side

As a first attempt towards biosensing, thiol's bonding at the gold-coated surface of the µCs was recorded by means of the Cantisens® Research system. The measured deflection results from the surface stress that is generated during the self-assembly of thiol molecules on the gold-coated substrate. Using the Stoney formula, the surface stress values can be uncovered to derive the sensitivity of the cantilever sensor. Figure 2 represents deflection curves of the six central cantilevers of a 60 µm-thin PVDF array. Although the curves have the expected characteristic behavior, the maximal amplitudes differ by up to a factor of three, which is mainly due to the variations of the µCs-geometry. Note the cantilever width, for example, varies from 80 and 130 µm.

4. Conclusions and Outlook

Injection molding permits the fabrication of polymeric micro-cantilever arrays with reasonable properties for biomedical applications. The choice of polymer and geometry allows tailoring sensor characteristics. The preliminary thiol binding tests demonstrate that polymeric Cs are highly sensitive surface stress monitors. The resonance frequencies of the polymeric Cs are higher than their silicon counterparts making them especially suitable for gas sensing. Recent studies have demonstrated the applicability of Cs as olfactory sensors [7,8]. Last year one of the first clinical studies was published applying standard silicon Cs for the detection of two diseases [8].

In addition, polymeric Cs can be used to measure contractile cell forces as described by Köser et al. [9]. Modifying its surface morphology or chemistry one can mimic implant surfaces and can compare the influence on the cell response in physical manner. Thus, the disposable C array sensors will support the selection of advanced surface-modified substrates and medical implant surfaces, along with opening more applications in the field of biomedicine.

Acknowledgements

This activity is funded by the Swiss Nanoscience Institute (SNI) through the applied research project DICANS, a collaborative initiative between the Biomaterials Science Center (BMC), Paul Scherrer Institut (PSI), University of Applied Sciences Northwestern Switzerland (FHNW) and Concentris GmbH. The authors would like to thank K. Jefimovs (EMPA Dübendorf) for the laser micro-machining of the mold and the members from the LMN-PSI for their technical assistance. The Solvay PEEK grades used in this study was kindly supplied by Bigler AG.

References

[1] Geoders K, Colton J, Bootomley L. Microcantilevers: sensing chemical interactions via mechanical motion. *Chem Rev* 2008;**108**:522–542.

[2] Berger R. Cantilever Sensors. *Development of Methods* 2008;**16**:119–120.

[3] Calleja M, Tamayo J, Johansson A, Rasmussen P, Lechuga L, Boisen A. Polymeric cantilever arrays for biosensing applications. *Sensor Lett* 2003;**1**:1-5

[4] Heckele M. Review on micro molding of thermoplastic polymers. *J Micromech Microengin*. 2004;**14**.

[5] Schift H, Bellini S, Pieles U, Gobrecht J. Sustained polymer membranes fabricated by nanoimprint lithography. *J Microlithography, Microfabrication and Microsystems* 2006;**5**.

[6] Schift H, David C, Gabriel M, Gobrecht J, Hyderman L, Kaiser W, Körpel S, Scandella L. Nanoreplication in polymers using hot embossing and injection molding. *Microelec Engin* 2000;**53**:171–174.

[7] Battiston F, Ramseyer J, Lang H, Baller M, Gerber C, Gimzewski J, Meyer E, Güntherodt J. A chemical sensor based on a microfabricated cantilever array with simultaneous resonance-frequency and bending readout. *Sensors and Actuators B* 2001;**77**.

[8] Schmid D, Lang H, Marsch S, Gerber C, Hunziker P. Diagnosing disease by nanomechanical olfactory sensors. *Eur J Nanomed* 2008;**1.**

[9] Köser J, Gobrecht J, Pieles U, Müller B. Detection of the forces and modulation of cell-substrate interactions. *Eur Cells Mater* 2008;**16:**38.

Sensors and Actuators A 172 (2011) 2–8

Contents lists available at ScienceDirect

Sensors and Actuators A: Physical

journal homepage: www.elsevier.com/locate/sna

Surface patterned polymer micro-cantilever arrays for sensing

Prabitha Urwyler[a,b,*], Helmut Schift[a], Jens Gobrecht[a], Oskar Häfeli[c], Mirco Altana[d], Felice Battiston[e], Bert Müller[b]

[a] Paul Scherrer Institut, Laboratory for Micro- and Nanotechnology, 5232 Villigen PSI, Switzerland
[b] University of Basel, Biomaterials Science Center, c/o University Hospital, 4031 Basel, Switzerland
[c] University of Applied Sciences Northwestern Switzerland, Institute of Polymer Engineering, 5210 Windisch, Switzerland
[d] University of Applied Sciences Northwestern Switzerland, Institute of Polymer Nanotechnology, 5210 Windisch, Switzerland
[e] Concentris GmbH, Davidsbodenstrasse 63, 4012 Basel, Switzerland

ARTICLE INFO

Article history:
Available online 16 December 2010

PACS:
81.16.Nd (nanolithography)
81.20.Hy (molding)
87.19.lt (sensory systems)
87.80.Ek (micromechanical techniques)
87.85.Rs (nanotechnology-applications)
87.85.dh (cells on a chip)

Keywords:
Micro-cantilever
Polymer
Sensor
Injection molding
Nanoimprint lithography
Stamps
Mold

ABSTRACT

Microinjection molding was employed to fabricate low-cost polymer cantilever arrays for sensor applications. Cantilevers with micrometer dimensions and aspect ratios as large as 10 were successfully manufactured from polymers, including polypropylene and polyvinylidenfluoride. The cantilevers perform similar to the established silicon cantilevers, with *Q*-factors in the range of 10–20. Static deflection of gold coated polymer cantilevers was characterized with heat cycling and self-assembled monolayer formation of mercaptohexanols. A hybrid mold concept allows easy modification of the surface topography, enabling customized mechanical properties of individual cantilevers. Combined with functionalization and surface patterning, the cantilever arrays are qualified for biomedical applications.

1. Introduction

Micro-cantilevers (μCs), similar to those used in scanning force microscopes (SFM), have become increasingly popular as transducers in chemical and biological sensors [1–8]. They convert physical, chemical, and biological stimuli into measurable signals. Various detection methods have been introduced to measure the bending of the μCs in the range of few nanometers with extremely high accuracy. A compelling feature of μC sensors is that they operate in air, vacuum, or liquid environment [7]. Like many micro-machined devices, μCs are typically made from glass, silicon or other rigid materials. In the field of biomedicine, silicon-based μCs have to be cleaned or even sterilized for repetitive use. For single usage they are often too expensive. The fabrication is based upon single crystalline silicon wafers to be processed in cleanroom facilities. The high costs compromise many applications and calls for low-cost, disposable sensing elements. Polymer materials offer tailored physical and chemical properties to be combined with low-cost mass production. Therefore, compared to silicon-based μCs the polymeric μCs can exhibit better biocompatibility and much better adaptability of rapid prototyping along with mechanical properties, which make them particularly sensitive [7]. Despite these advantages polymeric μC arrays are not yet commercially available. Polymer μCs can be prepared in a variety of ways, whereas the type of polymer often determines the fabrication method [7,9]. So far, polymer μCs were realized using photolithography. It is limited to the suitable materials and the μCs fabrication is rather expensive [10]. Molding of microcomponents from thermoplastic polymers has become a routinely used industrial production process and is one of the most promising fabrication techniques for non-electronic micro devices [11]. Fabrication costs of molded parts

* Corresponding author at: Paul Scherrer Institut, Laboratory for Micro- and Nanotechnology, ODRA 117, 5232 Villigen PSI, Switzerland. Tel.: +41 56 3102430.
E-mail addresses: prabitha.urwyler@psi.ch (P. Urwyler), helmut.schift@psi.ch (H. Schift), jens.gobrecht@psi.ch (J. Gobrecht), oskar.haefeli@fhnw.ch (O. Häfeli), mirco.altana@fhnw.ch (M. Altana), battiston@concentris.ch (F. Battiston), bert.mueller@unibas.ch (B. Müller).

0924-4247/$ – see front matter © 2011 Elsevier B.V. All rights reserved.
doi:10.1016/j.sna.2010.12.007

are hardly affected by the complexity of the design. Once a mold insert is available, several thousand parts can be molded with modest effort. Furthermore, different polymers can be used to obtain parts of almost identical shape with a high degree of reproducibility. Micro-patterns on the mold can be replicated into the molded device, too, making it possible to integrate different dimensions and topographies into one single tool. The mechanical properties of polymer μCs can be tailored choosing appropriate dimensions and surface morphologies. The cost of the raw material in most cases is negligibly low, because only small quantities are required for micrometer-sized components. Therefore, parts fabricated by micromolding, even from high-end materials, are suitable for applications requiring low-cost and disposable components. Several thermoplastic molding processes such as hot embossing, injection molding (IM), injection compression molding and thermoforming give rise to micro-parts with high precision and repeatability [11,12]. Polymeric replication techniques based on nanoimprint and casting of curable polymers can be used to produce structures with sub-100 nm resolutions [13,14]. The hot embossing and the IM seem to be the most industrially viable processes for molded micro-parts [15]. Polystyrene (PS) cantilever beams of thicknesses between 2 and 40 μm with a stiffness ranging from 0.01 to 10 N m^{-1} have been produced using IM [10]. The acceptance of μC sensors in research and commercial, analytic applications crucially depends on the robustness, the ease of use, the reproducibility and finally the price. The question arises if disposable polymeric μC arrays can be fabricated on the basis of standard thermal IM using precisely machined metal molds. It is the aim of the present scientific activities to adapt IM, well established on the millimeter scale and above, to molds with 30 μm-thin cavities, 500 μm long and 100 μm wide to realize polymer μCs with a performance comparable to the presently used silicon-based arrays (hence termed micro-injection molding (μIM)). Sensitivity enhancement using customized surface structuring within the mold cavity is also being studied.

2. Materials and methods

2.1. Comparing established rigid μCs with polymeric ones

μCs respond to impacts ranging from surface stress via mass change to temperature. Their sensing involves the detection of μC deflections and of μC resonance frequencies. The laser beam projection technique provides the μC deflection induced by the forces acting on the cantilever [4]. Forces in the pN-range are detectable, since the setup can uncover sub-nanometer deflections of the apex of the μC sensors. These forces comprise expansions or contractions acting on one side of the cantilever surface [16]. One applies static and dynamic modes for more or less sophisticated sensing. In static mode, the surface stress generated from selectively adsorbed molecules on one side of the cantilever is measured. The free-end deflection Δ_z as the result of the surface stress $\sigma_{surface}$ is often quantified using the well-known Stoney formula [4,7], for example in the form of Sader [17]:

$$\Delta_z = \frac{3(1-\nu)L^2}{Et^2}(\Delta\sigma_{surface}) \quad (1)$$

where $\Delta\sigma_{surface}$ is the difference of surface stress between top and bottom sides of the cantilever, ν is the Poisson's ratio and E is the Young's modulus of the cantilever material and L and t are the length and thickness of the cantilever, respectively.

In dynamic mode, the *resonance frequency* of the cantilever f_{res} is monitored during mass adsorption on the cantilever [18]. The related shifts in resonance frequency Δf_{res} are given for homogeneously distributed adsorbents by

$$\Delta f_{res} \approx -f_{res}\frac{\Delta m}{2m_0} \quad (2)$$

where Δm is the absorbed mass and m_0 is the initial mass of the cantilever [18]. The frequency shifts per mass change on the typically applied cantilever of rectangular shape is

$$\frac{\Delta f_{res}}{\Delta m_0} = \frac{1}{4\pi n_l L^3 w}\sqrt{\frac{E}{\rho^3}} \quad (3)$$

with $\rho = m/Lwt$ as mass density and $n_l \sim 1$ as characteristic geometrical μC parameter [1].

The frequencies for the ith resonance mode, f_i, can be estimated using the μC geometry, L and t, and the materials density ρ, 2330 and 3180 kg m^{-3} for Si and Si_3N_4 as well as 1220, 900, and 1220 kg m^{-3} for the polymers polyvinylidenfluoride (PVDF), polypropylene (PP), and polyoxymethylene copolymers (POM-C), respectively:

$$f_i = \frac{t}{2\pi}\left(\frac{\alpha_i}{L}\right)^2\sqrt{\frac{E}{12\rho}} \quad \alpha_i: \quad \alpha_1 = 1.9; \quad \alpha_2 = 4.7; \quad \alpha_3 = 7.8; \quad \ldots \quad (4)$$

α_i is a constant obtained by numerically solving the beam frequency equation [7]. The Q-factor characterizes the resonator's bandwidth B relative to its centre frequency and the μC damping δ during ring-off:

$$Q = f\frac{\pi}{\delta} = \frac{f}{B} \quad (5)$$

The sensitivity of the sensor depends on the mechanical parameters Young's modulus E, ~130–188 GPa for Si, 310 GPa for Si_3N_4, as well as 6.7, 1.9 and 6.7 GPa for PVDF, PP, and POM, respectively, and Poisson ratio $\nu \sim 0.22$ for Si and 0.24 for Si_3N_4 as well as 0.3–0.5 for most polymers. In order to fabricate polymer μCs with sensitivity comparable with silicon ones (typical dimensions of $L \sim 500$ μm and 1–5 μm thickness), while keeping L constant, the μCs have to be one order of magnitude thicker to compensate the hundred times smaller E.

For the selective sensitivity to detect contaminants in gases or dedicated species in liquids, the cantilever surfaces have to be functionalized. For this purpose, one μC side is coated or patterned to enhance selective binding of the species of interest chemically or by featured surface morphology. Chung et al. [16], for example, used field ion beam milling to build nanostructures on the μC surfaces. The mechanical properties of the μCs depend on the coating and its thickness as well as the morphological features including pattern sizes. Field ion beam milling modifications soften cantilevers [19,20], whereas corrugations generated by means of stencils stiffen cantilevers and membranes [21]. μIM belongs to the attractive approaches to manufacture polymer μC with pre-defined surface microstructures.

2.2. Microinjection molding

A modular injection molding tool has been developed that consists of a high quality steel cylinder (Polmax Uddeholm) 30 mm in diameter as mold insert with two internal resistive heating cartridges (Watlow Firerod, 230 V, 180 W, 49 W/cm^2) fixed in the three-plate molding tool 'handy mold' with ejector pins (see Fig. 1, left side). This setup enables us to proceed with both isothermal and variothermal heating schemes with short heating times for temperatures as high as 320 °C in the vicinity of the mold cavities. The tool is installed in the clamping unit of an Arburg 320 Allrounder (Arburg, Lossburg, Germany) with a maximum clamping force of 600 kN.

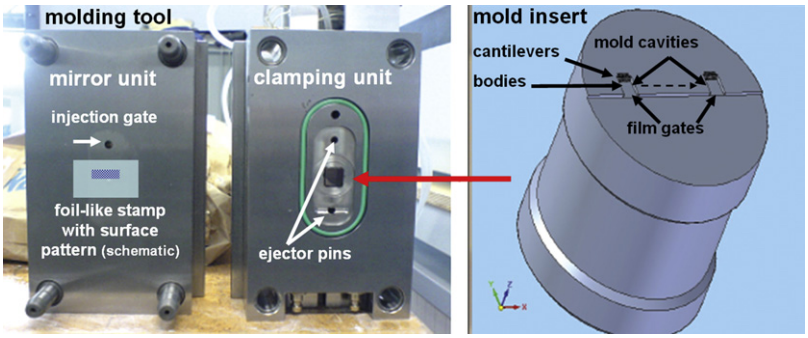

Fig. 1. Molding tool (handy mold) with two sides (left side). The mirror side contains the gate (top) and the location, where the patterned foil is placed. The clamping unit contains the mold insert (right side) with two mold cavities.

In contrast to the work of Andrew et al. [10] with one mold cavity composed of two halves placed in the opposite mold units of the IM machine to generate cantilevers with symmetric position, the present mold system comprises only one cavity located on the closing side [22,23]. The other side is free for mirror plates with designed micro- or nano-features.

The two parallel mold cavities (see Fig. 1, right side) were fabricated using laser ablation, and placed into the central part of the flat end of the cylinder. They are connected to the injection gate via a large plate-like cavity through 2.5 mm-wide gates for filling. The μC chip was designed with outlines of a micro-machined 500 μm-thick silicon μC with a $3.5 \times 2.5\ mm^2$ large body. It has eight 80–130 μm-wide μC beams with a 500 μm pitch on one side. The thickness chosen was usually in the range between 20 and 40 μm. To guarantee fast and complete filling also molds with 60 μm depths were applied (see Fig. 2, top micrograph). For the venting, at the end of each beam cavity thin, 5 mm-long, $10 \times 10\ \mu m^2$-wide channels were incorporated. The polished steel plate with one injection gate is the flat counterpart opposite to the closing unit. Therefore, the upper side of each μC beam has a polished finish (see Fig. 2, bottom micrograph) later used for laser beam reflection. Surface patterned beams require, thus, an additional mold insert with a micro- and nano-relief to be introduced at the mirror side. In place of another mold insert, we incorporate a thin, patterned polymer foil (see Fig. 1, left side). This foil-like mold prepared by hot embossing, typically 25–100 μm thick, forms the interface between the two units of the IM machine and is subjected to related pressure and heat. To ensure repeated alignment during injection and demolding, it is directly fixed onto the polished top by adhesive tape or clamps. The mold temperatures and pressures have to be low enough to enable a sufficient number of replications without degradation of the surface relief. The main advantage of the method lies in the simple integration of gratings with different sizes and orientations. It is particularly useful for test series. Even for mass production the method is promising, since polymer foils can be patterned in roll-to-roll processes [24,25].

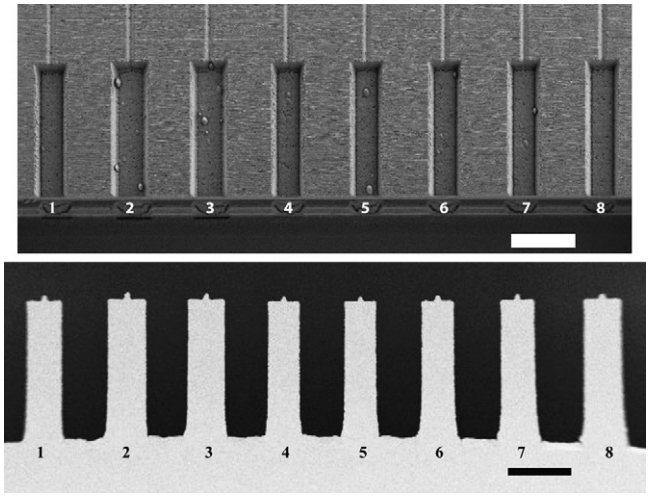

Fig. 2. The top SEM micrograph shows the array of eight laser ablated cantilever cavities in the steel mold insert. The cavity width varies from 80 to 130 μm. The scale bar corresponds to 200 μm. The SEM micrograph on the bottom is an image of an injection molded PP micro-cantilever array. Small tips at the cantilever end demonstrate the complete filling up to the venting channels.

2.3. Microinjection molded polymer materials

The polymers used are different grades of poly(etheretherketone) (PEEK: Solvay Advanced Polymer AvaSpire AV-650 BG15, Solvay Advanced Polymer KetaSpire KT-880NT, Victrex 150G), poly(propylene) (PP: Moplen SM 6100), polyoxymethylene copolymers (POM-C: 511P Delrin NC010), cyclic olefin copolymers (COC: Topas 8007X10), polyvinylidenfluoride (PVDF: Kynar 720 Arkema) and liquid crystal polymer (LCP: Vectra A 390).

2.4. Microinjection mold processes

Up to 160 °C, the tool temperatures were controlled by heated water. For the higher process temperatures up to 260 °C oil served as heat transport medium. The other process parameters are summarized in Table 1. As the foil mentioned above 100 μm-thick polycarbonate (PC: Bayer Makrofol ID 6-2) and 25 μm-thick PEEK (Aptiv 2000 series) were inserted. While PC with a glass transition temperature of 148 °C only allows molding polymers with rather low process temperatures, PEEK, which has a comparative glass transition temperature of 143 °C was considered as higher temperature alternative because of its excellent demolding properties. The PC and PEEK foils were hot embossed in a Jenoptik HEX 03 machine for a period of 10 min using temperatures of 160 and 175 °C and forces of 15 and 4 kN, respectively. As the molds for hot embossing, either surface patterned silicon wafers or replicas in Ormostamp both with anti-sticking layer were used [26,27].

Table 1
Injection molding process parameters for the selected polymer materials including all grades of PEEK.

	COC	PP	PEEK	POM-C	LCP	PVDP
Melt temperature [°C]	240	200	400	220	300	220
Tool temperature [°C]	77	40	225	120	150	120
Mold insert temperature [°C]	77	40	260	120	150	120
Injection speed [cm^3/s]	30	9	10	10	10	10

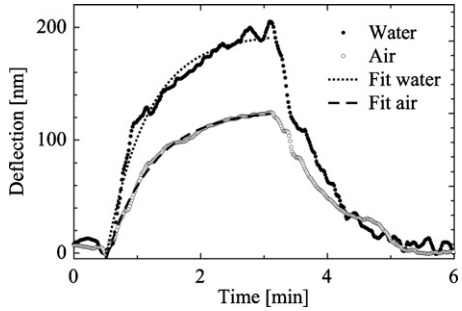

Fig. 3. Real time monitoring of injection molded PVDF μC deflection: heat test of 30 μm-thick μCs with a temperature increase from 25 to 35 °C at a heating rate of about t_{heat} = 0.5 min and a temperature decrease back to 25 °C at a cooling rate of about t_{cool} = 3.2 min.

2.5. Cantilever finishing

The injection molded μCs were coated on the mirror side with 20 nm-thin gold films using a thermal evaporator (Balzers BAE250). This film guarantees sufficient laser beam reflectivity to use the Cantisens® research system (Concentris GmbH, Basel, Switzerland) for measuring the deflection and the resonance frequency of the μC. Replication quality was analyzed using scanning electron microscopy (SEM: Supra 55 VP, Carl Zeiss NTS GmbH, Oberkochen, Germany), after coating with a thin layer of PdAu.

3. Results

Complete filling of the mold cavities was observed for all polymers using isothermal μIM (Fig. 2, bottom micrograph for PP) with the exception of the high-performance polymer PEEK, which requires mold temperatures of up to 320 °C and processing temperatures higher than 260 °C. We have not observed any degradation for PP, COC, POM-C, and PVDF. However, with PEEK, which is more sensitive to longer residence time, visible signs of degradation were observed. Also with the patterned foil-like molds, using standard isothermal μIM process parameters, a complete filling of high-aspect-ratio micro-cavities was achieved for PP (see Fig. 5). The mold temperature was low enough to use the polymeric foils for several hundreds replications without degradation of the surface relief.

With the exception of PEEK, the cantilevers reveal the expected thermal behavior as demonstrated in the diagram in Fig. 3 for the gold-coated PVDF cantilever under atmospheric conditions, i.e. in air, and in liquid (water). The heat tests included a temperature cycle with an increase from 25 to 35 °C and a subsequent decrease back to 25 °C within a time of about 4 min. The heat tests prove the sensitivity of the cantilevers that corresponds to deflections of the order of 10 nm. The deflection signal exhibits an exponential, asymptotic behavior as confirmed by the fits in Fig. 3. For the temperature difference of 10 K the maximal deflection for PVDF μCs in air corresponds to (95 ± 16) nm and (55 ± 5) nm for thicknesses of 30 μm and 40 μm, respectively. In water, these values should be similar but gave higher values, namely (127 ± 17) nm and (154 ± 55) nm. Note the larger scattering of the data in liquid, which indicates less stable experimental conditions and reduced reproducibility in liquid compared to air.

The Cantisens® Research system permits the experimental determination of resonance frequencies f_{res} and quality factors Q for the polymeric μCs. Table 2 summarizes the mean values and related standard deviations of the resonance frequency measurements for the μCs in air and water. The deviations of the experimental data from the estimated ones are reasonably explained accounting for dimensional variations as well as the frequency dependence on E.

Table 2
Mean values and related standard deviations of the resonance frequency f_{res} as well as quality factor Q in air and water.

μC thickness and polymer	30 μm PP	40 μm PP	30 μm PVDF	40 μm PVDF	30 μm POM-C
f_{res} in air (experimental) [kHz]	48 ± 3	50 ± 1	60 ± 3	79 ± 5	60 ± 4
f_{res} (theoretical, Eq. (4))	38	46	66	88	78
f_{res} in water (experimental) [kHz]	37 ± 8	33 ± 27	43 ± 5	52 ± 5	36 ± 7
Q-factor in air	28	46	38	19	33
Q-factor in water	20	11	10	9	19

The drop in resonance frequency in water results from the damping, which lowers the Q-factor of the μCs as given in Table 2. The Q-factors were estimated directly from the frequency spectra [1,2,4].

The stiffness of the μCs was determined by nanoindentation of the injection molded PP μCs. The measurements were carried out using a nanoindenter (MTS XP® with a Berkovich tip (XPT-12761-0)). The unloading segment of the measured load–displacement curve in nanoindentation permits an estimation of the cantilever's Young's modulus, by defining the elastic stiffness as the slope of the unloading segment [28]. The obtained value of 2.4 GPa is close to the value (1.9 GPa) mentioned in the technical datasheet from the PP supplier.

As a first attempt towards biosensing, the chemisorption of thiols on gold coated μCs was recorded by means of the Cantisens® Research system. The data of six PVDF 60 μm-thick μCs from an injection molded array are shown in the diagram of Fig. 4. The deflection results from the surface stress, that is generated during the self-assembly of thiol molecules on the gold-coated substrate. Using the Stoney formula (1), the surface stress values can be determined to derive the sensitivity of the individual μC sensors. Although the curves in Fig. 4 exhibit the expected characteristic behavior, the maximal amplitudes differ by up to a factor of three.

3D corrugation patterns have been applied to enhance the stability of membranes and their stiffness against bending [21]. Therefore, 5 μm-wide stripes as presented in Fig. 5 were introduced into the mold and tested for cantilevers, too. Preliminary experiments show that 5 μm-deep trenches, when oriented parallel to the beam, enhance the resonance frequency, and also serve as a means to stiffen cantilevers against torsion (see Fig. 6). For separation of different patterns, only a rough alignment of the stripe patterns needs to be ensured. However, as can be seen in Fig. 6, due to the softening of the polymer mold during injection, the venting channels can be closed, leading to an incomplete filling of the mold cavities. This seems more likely with 1 μm-deep stripes in Fig. 6, particularly if they are oriented perpendicularly and not parallel to the beam.

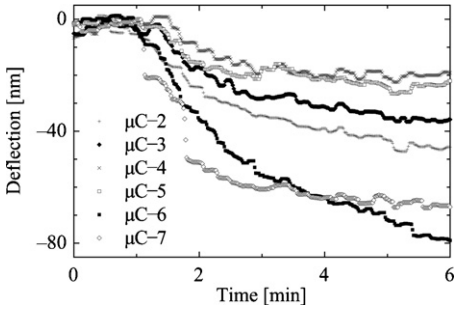

Fig. 4. Real-time monitoring of injection molded PVDF μC deflection in static mode. Formation of mercaptohexanol self-assembled monolayers on gold-coated 60 μm-thick μCs.

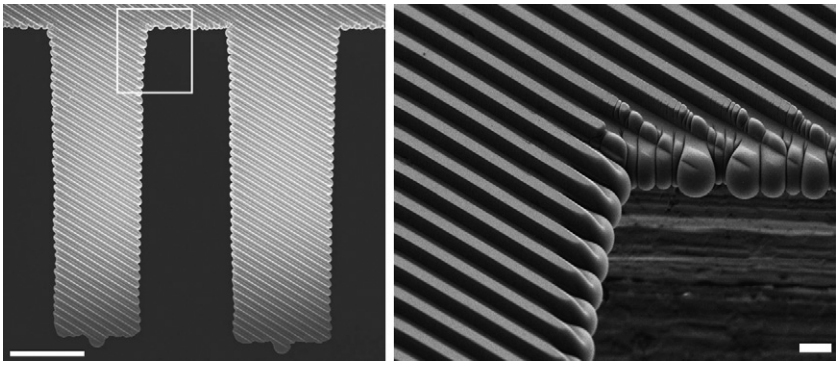

Fig. 5. SEM micrographs of the line pattern (period 10 μm, depth 5 μm, width 5 μm) transferred during the μIM process from a foil-like mold to the surface of two molded μC (left side). In contrast to the non-patterned original beams, the surface patterned beams are slightly (10%) wider due to high injection pressure and the softness of the PC foil (see extract at right side). The scale bar for the left micrograph corresponds to 100 μm and right micrograph corresponds to 10 μm.

4. Discussion

The incorporation of a foil-like mold with well-defined microstructures into the molding tool is a relatively simple approach to build microstructures on the polymer cantilevers. One can easily change the design, the size and the orientation of the pattern as demonstrated by the micrographs in Figs. 5 and 6. The orientation of the lines along the μCs is controlled without changing the device dimensions and outlines. Deep longitudinal stripes aligned within 5 μm precision promote the complete filling of the mold cavities and, hence, give rise to fully molded cantilevers. Moreover, these longitudinal channels are preferred for the contractile cell force measurements [29] as cells generally orient themselves along the ridges. Deep trenches with directions perpendicular to the beams can lead to a slight broadening of the cantilever, since material can flow in the trenches of the softened foil-like mold during injection. Different orientations, depths and patterns will be tested in future.

The differences of the heat tests in water and air are associated with an artifact, which results from the optical refraction at the air–water interface in the Concentris system. This also explains the larger data scattering. However, the main reason for the large tolerances observed in the experimental data is due to the fact the current mold exhibits large dimensional variations and a large surface roughness. The latter may be responsible that during demolding, high demolding forces induce intrinsic stress and distortion. This will be improved by using molds with reduced surface roughness.

The thiol adsorption measurements elucidate the necessity of calibration before reproducible experiments can be performed. As noted before, the deflection variations between the cantilevers originate mainly from the discrepancies in the μCs geometry. Consequently, the processing has to be improved or, alternatively, the obtained μCs have to be precisely calibrated in a more or less individual fashion.

5. Conclusions and outlook

μIM permits the fabrication of polymeric μC arrays with fair properties for biomedical applications. The choice of polymer material and geometry allows tailoring the sensor characteristics. The thiol-gold binding tests demonstrate that the prepared polymer μCs are highly sensitive surface stress monitors. Recent studies have demonstrated the applicability of μCs as olfactory sensors [30,31]. Last year one of the first clinical studies was published applying standard silicon μCs for the detection of diseases [31]. In addition, polymer μCs can be used to measure contractile cell forces [29]. By modifying its surface morphology or chemistry one can mimic implant surfaces and can compare the influence on the cell response. Thus, the microstructured μC array sensors will support the selection of advanced surface-modified substrates and medical implant surfaces.

Initial mechanical and functional tests imply that these polymer μCs are mechanically compliant for use in biochemistry and biomedicine. An additional advantage is that the polymer cantilevers can be modified adding micro- and nano-patterns to the mold cavities [32–34]. It is expected that by choosing appropriate sizes and orientations of the surface microstructures, the mechanical properties of individual μCs with identical outlines can be modified, e.g. by softening (line ridges perpendicular to beam) or stiffening (line ridges along beam) of the beam. Surface structuring can also tailor cell locomotion, adhesion and spreading, which are closely related to the contractile cell forces to be quantified. The

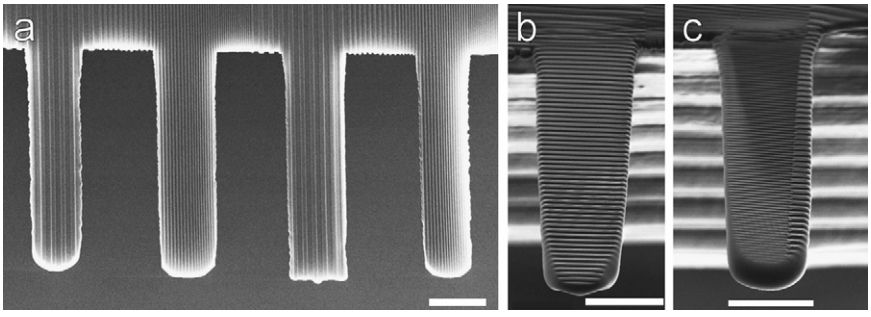

Fig. 6. SEM micrographs of PP μCs line patterns (depth 1 μm) (a) with different periods in the direction of beams and (b), (c) perpendicular to beams (right side), (c) with two patterns on one beam. The scale bars corresponds to 100 μm.

μCs patterning can be established for a range of cantilever designs. Once successfully established, the polymer-based μC systems will permit to gain major cost reductions and to address further applications in the field of biomedicine.

Acknowledgement

This activity is funded by the Swiss Nanoscience Institute (SNI) through the applied research project DICANS, a collaborative initiative between the Biomaterials Science Center (BMC) of the University of Basel, Paul Scherrer Institut (PSI), University of Applied Sciences Northwestern Switzerland (FHNW) and Concentris GmbH. The authors would like to thank K. Jefimovs (EMPA Dübendorf) for the laser micro-machining of the mold, R. Ghisleni (EMPA Thun) for his assistance with the MTS XP® system, J. Köser (FHNW Muttenz) for his advice on using the Cantisens® research system and the members from the LMN-PSI, for their technical assistance. The Solvay PEEK grades used in this study was kindly supplied by Bigler AG. The MTS XP® system used in this study is maintained and operated by EMPA Thun.

References

[1] H.P. Lang, M. Hegner, Ch. Gerber, Nanomechanical cantilever array sensors, in: B. Bhushan (Ed.), Handbook of Nanotechnology, Springer Verlag, Berlin/Heidelberg, 2010, pp. 427–452.
[2] B. Bhushan, O. Marti, Scanning probe microscopy – principle of operation, instrumentation, and probes, in: B. Bhushan (Ed.), Handbook of Nanotechnology, Springer Verlag, Berlin/Heidelberg, 2010, pp. 573–617.
[3] D. Lange, O. Brand, H. Baltes, CMOS cantilever sensor systems, atomic-force microscopy and gas sensing applications, in: Microtechnology and MEMS VIII, 2002, p. 150.
[4] R. Berger, Ch. Gerber, H.P. Lang, J.K. Gimzewski, Micromechanics: a toolbox for femtoscale science: "towards a laboratory on a tip", Microelectron. Eng. 35 (1997) 373–379.
[5] H.P. Lang, R. Berger, F. Battiston, J.-P. Ramseyer, E. Meyer, C. Andreoli, J. Brugger, P. Vettiger, M. Despont, T. Mezzacasa, L. Scandella, H.-J. Güntherodt, Ch. Gerber, J.K. Gimzewski, A chemical sensor based on a micromechanical cantilever array for the identification of gases and vapors, Appl. Phys. A 66 (1998) S61–S64.
[6] M. Toda, Y. Joseph, R. Berger, Swelling of Composite Films at Interfaces, J. Physical Chemistry C 114 (2010) 2012–2017.
[7] K. Geoders, J. Colton, L. Bootomley, Microcantilevers: sensing chemical interactions via mechanical motion, Chem. Rev. 108 (2008) 522–542.
[8] A. Vidic, D. Then, Ch. Ziegler, A new cantilever system for gas and liquid sensing, Ultramicroscopy 97 (2003) 407–416.
[9] G. Genolet, M. Despont, P. Vettiger, D. Anselmetti, All-photoplastic, soft cantilever cassette probe for scanning force microscopy, J. Vac. Sci. Technol. B 18 (2) (2000) 617–620.
[10] M.A.P. Andrew, W. McFarland, L.A. Bottomley, J.S. Colton, Injection moulding of high aspect ratio micron-scale thickness polymeric microcantilevers, Nanotechnology 15 (2004) 1628–1632.
[11] M. Heckele, Review on micro molding of thermoplastic polymers, J. Micromech. Microeng. 14 (2004) R1–R14.
[12] J. Giboz, T. Copponnex, P. Mélé, Microinjection molding of thermoplastic polymers: a review, J. Micromech. Microeng. 17 (2007) 96–109.
[13] H. Schift, S. Bellini, J. Gobrecht, Perforated polymer membranes fabricated by nanoimprint lithography, Microelectron. Eng. 83 (2006) 873–875.
[14] H. Schift, S. Bellini, U. Pieles, J. Gobrecht, Sustained polymer membranes fabricated by nanoimprint lithography, J. Microlith. Microfab. Microsyst. 5 (2006) 011010.
[15] H. Schift, C. David, M. Gabriel, J. Gobrecht, L. Hyderman, W. Kaiser, S. Körpel, L. Scandella, Nanoreplication in polymers using hot embossing and injection molding, Microelectron. Eng. 53 (2000) 171–174.
[16] E. Chung, N. Lavrik, P. Datskos, J. Mcfarlane, S. Dai, C. Tsouris, Microcantilever sensors with chemically selective coatings of ionic liquids, AIChE J. 53 (10) (2007) 2726–2731.
[17] M. Calleja, J. Tamayo, L.M. Lechuga, A. Boisen, Highly sensitive polymer-based cantilever-sensors for DNA detection, Ultramicroscopy 105 (2005) 215–222.
[18] S.K.M. Nordström, M. Lillemose, A. Johansson, S. Dohn, D. Haefliger, G. Blagoi, M. Havsteen-Jakobsen, A. Boisen, SU-8 cantilevers for bio/chemical sensing; fabrication, characterisation and development of novel read-out methods, Sensors 8 (2008) 1595–1612.
[19] J.-H. Fabian, L. Scandella, H. Fuhrmann, R. Berger, T. Mezzacasa, Ch. Musil, J. Gobrecht, E. Meyer, Finite element calculations and fabrication of cantilever sensors for nanoscale detection, Ultramicroscopy 82 (2000) 69–77.
[20] J.-H. Fabian, L. Scandella, T. Mezzacasa, D. Bächle, J. Gobrecht, P. Lerch, E. Meyer, Fabrication of micromechanical cantilever sensors for nanoscale thermal detection, Ultramicroscopy 83 (2000) 873–875.
[21] M.A.F. van den Boogaart, M. Lishchynska, L.M. Doeswijk, J.C. Greer, J. Brugger, Corrugated membranes for improved pattern definition with micro/nanostencil lithography, Sens. Actuators A: Phys. 130–131 (2006) 568–574.
[22] P. Urwyler, O. Häfeli, H. Schift, J. Gobrecht, B. Müller, Disposable polymeric micro-cantilever arrays for biomedical applications, Eur. Cells Mater. 20 (2010) 48.
[23] P. Urwyler, O. Haefeli, H. Schift, J. Gobrecht, F. Battiston, B. Müller, Disposable polymeric micro-cantilever arrays for sensing, in: Proc. Eurosensors XX1V, September 5–8, Linz, Austria, 2010.
[24] H. Schift, Roll embossing and roller imprint, in: Y. Hirai (Ed.), Science and New Technology in Nanoimprint, Frontier Publishing Co Ltd, Japan, 2006, pp. 74–89.
[25] T. Mäkelä, T. Haatainen, P. Majander, J. Ahopelto, V. Lambertini, Continuous double-sided roll-to-roll imprinting of polymer film, Jpn. J. Appl. Phys. 47 (6) (2008) 5142–5144.
[26] H. Schift, Nanoimprint lithography: an old story in modern times? A review, J. Vac. Sci. Technol. B 26 (2) (2008) 458–480.
[27] H. Schift, C. Spreu, M. Saidani, M. Bednarzik, J. Gobrecht, A. Klukowska, F. Reuther, G. Gruetzner, H.H. Solak, Transparent hybrid polymer stamp copies with sub-50 nm resolution for thermal and UV-nanoimprint lithography, J. Vac. Sci. Technol. B 27 (6) (2009) 2846–2849.
[28] S.R. Kalidindi, S. Pathak, Determination of the effective zero-point and the extraction of spherical nanoindentation stress–strain curves, Acta Mater. 56 (2008) 3533–3542.
[29] J. Köser, J. Gobrecht, U. Pieles, B. Müller, Detection of the forces and modulation of cell–substrate interactions, Eur. Cells Mater. 16 (2008) 38.
[30] F. Battiston, J. Ramseyer, H.P. Lang, M. Baller, Ch. Gerber, J. Gimzewski, E. Meyer, J. Güntherodt, A chemical sensor based on a microfabricated cantilever array with simultaneous resonance-frequency and bending readout, Sens. Actuators B 77 (2001) 122.
[31] D. Schmid, H. Lang, S. Marsch, Ch. Gerber, P. Hunziker, Diagnosing disease by nanomechanical olfactory sensors, Eur. J. Nanomed. 1 (2008) 44.
[32] V. Seena, N.S. Kale, S. Mukherji, V. Ramgopal Rao, Development of polymeric microcantilevers with novel transduction schemes for biosensing applications, Solid State Sci. 11 (9) (2009) 1606–1611.
[33] J. Plaza, Villanueva, C. Domingeuz, Novel cantilever design with high control of the mechanical performance, Microelectron. Eng. 84 (5–8) (2007) 1292–1295.
[34] X.R. Zhang, X. Xua, Development of a biosensor based on laser-fabricated polymer microcantilevers, Appl. Phys. Lett. 85 (12) (2004) 2423–2425.

Biographies

Prabitha Urwyler received her Bachelor of Technology (B.Tech.) in Computer Engineering from the Mangalore University, India in 1995. She worked as a software engineer at Melstar Information Technologies Ltd, India from 1995 to 1997 and later at the Swiss News Agency (SDA–ATS), Switzerland until 2008. She pursued her masters in 2006, which earned her M.Sc. in Biomedical Engineering from the University of Bern in 2008. She is currently working towards her PhD degree in Biomedical Engineering on the fabrication, characterization and application of disposable micro-cantilevers for biomedical applications at the University of Basel and the Paul Scherrer Institut.

Helmut Schift received his diploma in Electrical Engineering from the University of Karlsruhe, Germany. He performed his Ph.D. studies at the Institute of Microtechnology Mainz (IMM), Germany. After his graduation in 1994, he joined PSI as a research staff member and is now head of the INKA-PSI Group in the Laboratory for Micro- and Nanotechnology at the PSI. He is actively involved in the development of nanoimprint lithography (NIL) as an alternative nanopatterning method for device fabrication. He is currently working in various national and international projects on stamp fabrication, hybrid technologies and innovative 3-D nanomolding.

Jens Gobrecht studied physics at the Technical University of Berlin, and received his diploma in engineering in 1976, followed by his Ph.D. from the Fritz-Haber Institut of the Max-Planck Society in Berlin. In 1980/1981 he worked on a post-doc position at the National Renewable Energy Laboratory in Golden, USA. After that he worked for 12 years in various functions at the ABB Corporate Research Center in Baden, Switzerland. In 1993 he joined the PSI and created the Laboratory for Micro- and Nanotechnology. In 2005 he was appointed Professor at the University of Applied Sciences of Northwestern Switzerland (FHNW) and head of the Institute of Polymer Nanotechnology (INKA), a joint venture with PSI. In 2007 J. Gobrecht co-founded "Eulitha AG", a company active in EUV-based nanolithography.

Oskar Hafeli received his diploma in tool design and construction in 1972. Since 1977, he is the chief of the Injection Molding laboratory at the Institute for Polymer Engineering (IKT) at FHNW. He is actively involved in disseminating education, supervising various bachelor, master and Ph.D. Thesis. His current work also includes research and development in the field of composites, natural fibers, micro- and nanoreplication for medical technology.

Mirco Altana received his diploma in Mechanical Engineering from the University of Applied Sciences Northwestern Switzerland in 2006. Currently he is pursuing his masters in Micro- and Nanotechnology at the University of Applied Sciences Vorarlberg in Dornbirn, Austria. He is working as a scientific assistant at the Institute of Polymer Nanotechnology (INKA) specializing in surface functionalization using nanoimprint lithography (NIL) and polymer functionalization.

Felice Battiston holds a degree in Electrical and Electronics Engineering and got a Ph.D. in Physics from the University of Basel in 1999. He worked as a post-doc at the University of Basel. Currently, he is the CTO of Concentris GmbH, which he founded in 2000.

Bert Müller received a diploma in mechanical engineering (1982), followed by the M.Sc. degree from the Dresden University of Technology and the Ph.D. from the University of Hannover, Germany in 1989 and 1994. From 1994 to 2001, he worked as a researcher at the Paderborn University, Germany, EPF Lausanne, ETH Zurich. He became a faculty member of the Physics Department at ETH Zurich in April 2001. After his election as Thomas Straumann-Chair for Materials Science in Medicine at the University of Basel, Switzerland and his appointment at the Surgery Department of the University Hospital Basel in September 2006, he founded the Biomaterials Science Center. He also teaches physics and materials science at the ETH Zurich and the Universities of Basel and Bern.

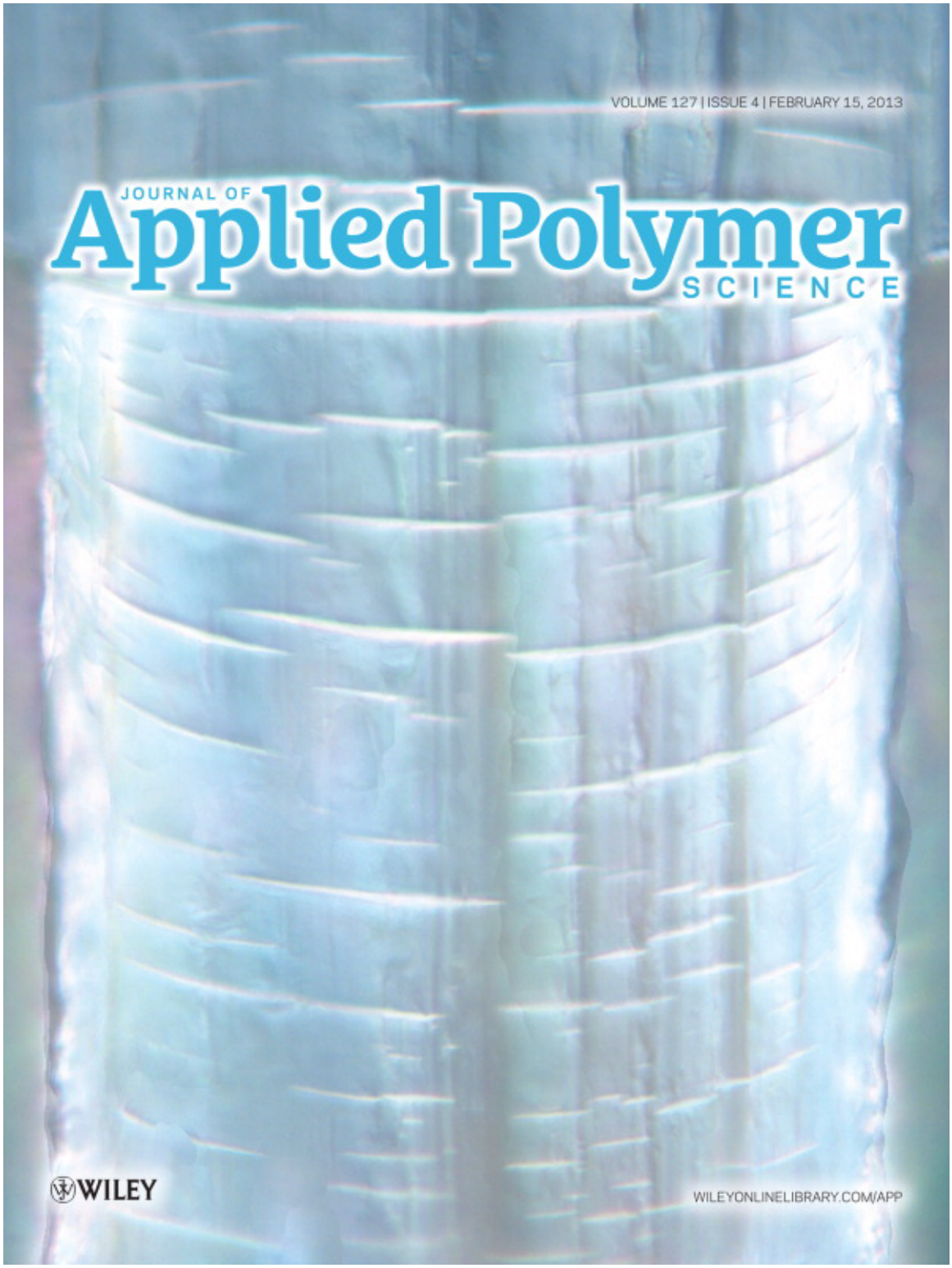
VOLUME 127 | ISSUE 4 | FEBRUARY 15, 2013
JOURNAL OF
Applied Polymer
SCIENCE
WILEY
WILEYONLINELIBRARY.COM/APP

JOURNAL OF Applied Polymer SCIENCE

Mechanical and Chemical Stability of Injection-Molded Microcantilevers Used for Sensing

Prabitha Urwyler,[1,2] Alfons Pascual,[3] Per Magnus Kristiansen,[3,4] Jens Gobrecht,[1,4] Bert Müller,[2] Helmut Schift[1,4]

[1]Paul Scherrer Institut, Laboratory for Micro- and Nanotechnology, 5232 Villigen PSI, Switzerland
[2]University of Basel, Biomaterials Science Center, c/o University Hospital, 4031 Basel, Switzerland
[3]University of Applied Sciences and Arts Northwestern Switzerland FHNW, Institute of Polymer Engineering, 5210 Windisch, Switzerland
[4]University of Applied Sciences and Arts Northwestern Switzerland FHNW, Institute of Polymer Nanotechnology, 5210 Windisch, Switzerland

Correspondence to: H. Schift (E-mail: helmut.schift@psi.ch)

ABSTRACT: Ultraviolet-ozone treatment is used as a standard surface cleaning procedure for removal of molecular organic contamination from analytical and sensing devices. Here, it is applied for injection-molded polymer microcantilevers before characterization and sensing experiments. This article examines the effects of the surface cleaning process using commercial equipment, in particular on the performance and mechanical properties of the cantilevers. It can be shown that the first chemical aging process essentially consist of the cross linking of the polymer chains together with a physical aging of the material. For longer exposure, the expected thermo-oxidative formation of carbonyl groups sets in and an exposure dependent chemical degradation can be detected. A process time of 20 min was found suitable as a trade-off between cleaning and stability. © 2012 Wiley Periodicals, Inc. J. Appl. Polym. Sci. 127: 2363–2370, 2013

KEYWORDS: microcantilever; polymer; injection molding; ultraviolet; ozone; degradation; polypropylene

Received 23 December 2011; accepted 15 March 2012; published online 9 May 2012
DOI: 10.1002/app.37767

INTRODUCTION

Disposable lab ware is essential in contemporary laboratory life. It is cost effective and meets the hygiene criteria. such as low microbiological contamination and ease of sterilization. Today, polystyrene (PS) and polypropylene (PP) are the most common polymers for such lab ware.[1] Recently, polymers have successfully entered the area of bioanalytics and -sensing. Mass production processes, including injection molding, have increasingly been used to manufacture products with microscopic dimensions, such as microfluidic platforms and diffractive optical elements.[2,3]

Microcantilevers (μCs), similar to those used in scanning force microscopy (SFM), have become popular as transducers in chemical and biological sensors.[4] In general, silicon technology was applied to produce these μC arrays. Due to growing interests in disposable devices in the life science sector, several manufacturing processes, including microinjection molding (μIM), have been developed to replace the rather expensive Si elements with polymeric ones.[3,5–9] Polymer materials offer tailored physical and chemical properties combined with low-cost mass production. Various polymers have been used to manufacture μCs using μIM. To ensure that polymeric μCs can be successfully applied under identical conditions, it has to be confirmed that the necessary cleaning procedures do not impair the μC's characteristics.

Cantilevers sense surface stresses transducing them into a bending, which is readily detected by laser deflection as in SFM systems. Surface selectivity toward biomolecules of interest is achieved by functionalizing cantilevers on one surface by immobilization of functional reagents (receptors). μCs are often gold coated to take advantage of thiol chemistry. Such thin gold films are also deposited on one side of the cantilevers to provide the necessary reflectivity for optical read-out.

A well-defined, homogeneously cleaned surface is a prerequisite for reproducible μC sensing. Organic contaminants not only impair receptor immobilization on cantilever surfaces but also affect the signal response of μCs and thus have to be removed according to suitable cleaning protocols. Plasma and ultraviolet-

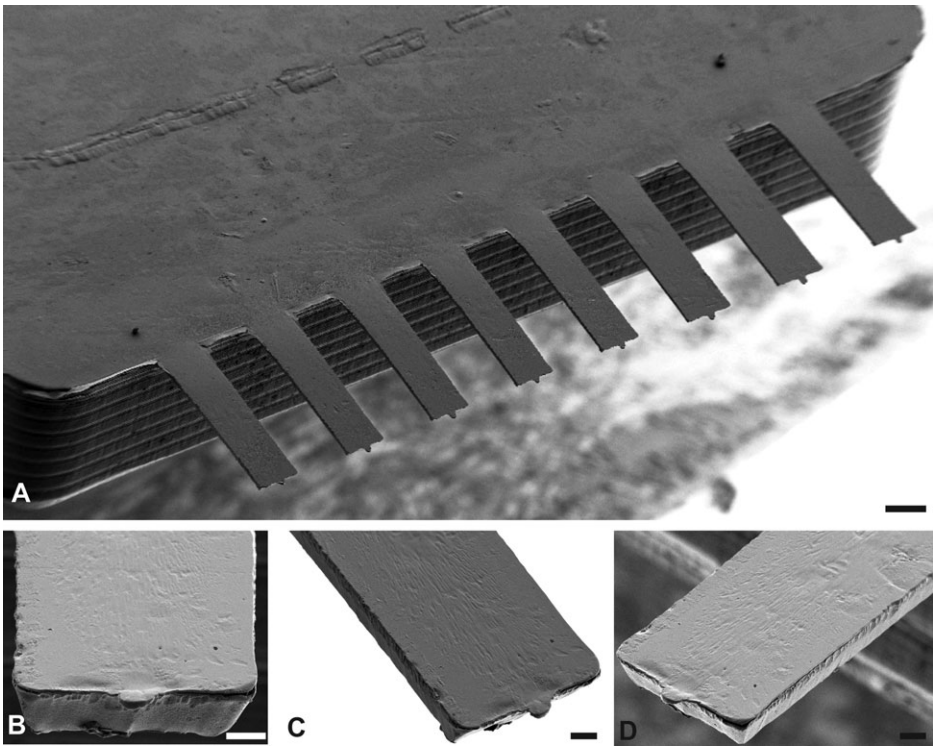

Figure 1. SEM micrograph of injection-molded PP μC with dimensions of 480 μm length, 80–130 μm width, and 30–36 μm thickness, showing outlines of the μC and part of the holder. The injection takes place from the holder into the cantilevers. Scale bar (A) 100 μm and (B–D) 20 μm.

ozone (UVO) treatments belong to the common dry cleaning procedures. In such plasma cleaning, the contaminants are removed using a combination of chemical reactions and physical, ballistic impact of gas molecules. Despite the straightforward application of plasma treatment, the availability of required vacuum systems limits the use in numerous laboratories. UVO treatment can be carried out at ambient conditions and, can thus be applied nearly everywhere. The mechanism behind UVO cleaning is a photosensitized oxidation process in which the contaminant molecules are dissociated by the absorption of UV light.[10] In addition, UV light converts atmospheric oxygen into reactive ozone. Ozone attacks the smaller fragments and thereby creates volatile organics, which desorb from the surface.[10] Consequently, UVO cleaning effectively removes the organic contaminants. Commercially available silicon μCs are regularly cleaned taking advantage of an UVO treatment for a period of 50 min.[11]

The surface of polymeric μCs, however, is also attacked by the UVO treatment, a process that may lead to undesired degradation. The rate of polymer degradation depends on the chemical composition. The latter not only determines the susceptibility to damage by incident irradiation (spectral sensitivity) but also paths of thermo-oxidative degradation and reactivity toward aggressive media, such as ozone and other atmospheric pollutants.[12] The combined impact of UV irradiation and oxygen generally causes chain scission reducing the mechanical and surface properties of the polymers, which could finally lead to device failure. Furthermore, the glass transition temperature of UVO-treated polymers is severely changed.[13]

The morphology of the injection-molded polymeric μCs strongly influences the sensitivity to degradation and deformation potential. Particularly, the amorphous skin layer which results from rapid cooling on contact with the mold is more prone to degradation than the bulk of the cantilever.[14] These factors determine whether the organic contaminants can be removed from polymeric μC surfaces before degradation and concomitant deterioration of the mechanical properties occurs. Hence, there is the need to investigate the effects of UVO treatment on polymeric cantilevers bearing in mind the need for a compromise between surface decontamination and cantilever maintenance. This is done through identification of appropriate treatments and exposure times to which injection-molded polymeric μCs could be subjected.

EXPERIMENTAL

Cantilever Manufacture

Polymeric μCs were produced using a modular injection molding tool as described previously.[8,9] The molding tool is installed in an Arburg 320 Allrounder (Arburg, Lossburg, Germany) with a maximum clamping force of 600 kN. The mirror unit of the molding tool, a polished steel surface ensured an optically flat and smooth surface. The μC array was designed with outlines of a micromachined 500 μm-thick silicon μC array with a 3.5 mm $\times$ 2.5 mm large body (holder). It has eight 480 μm long and 80–130 μm-wide μC beams as shown in Figure 1(A). The μC mold cavity depth was in the range between 30 and 36 μm. Due to the laser ablation process, the cross section of the μC is trapezoidal as shown in Figure 1(B). The width of the

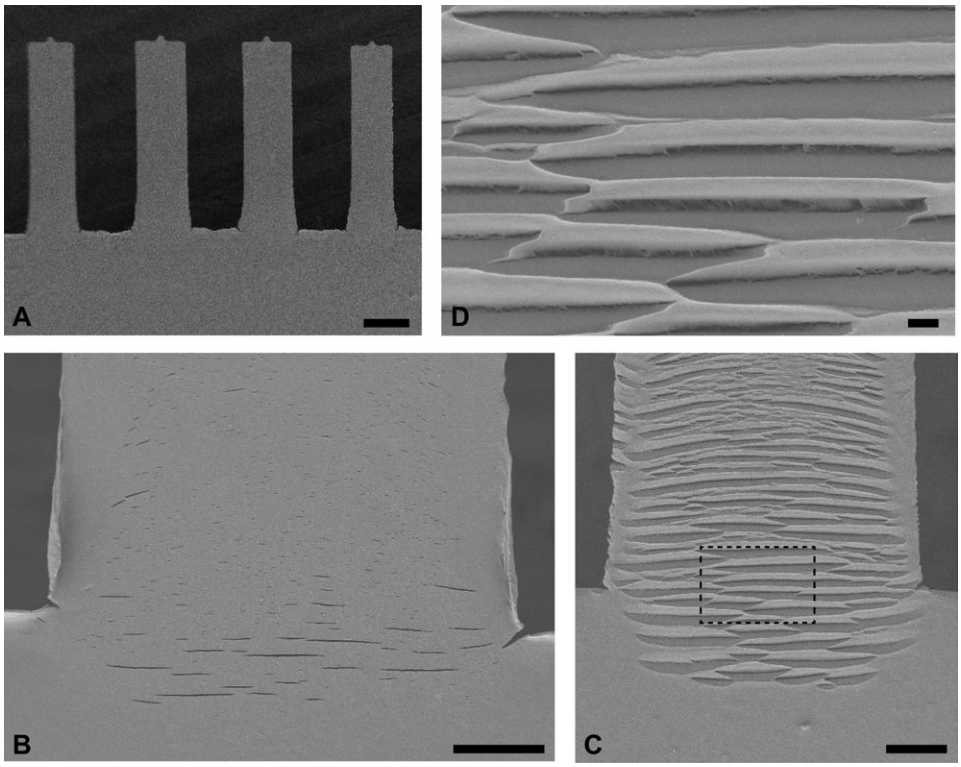

Figure 2. SEM observation of surface damage evolution with the UVO exposure: (A) 30 min, (B) 60 min, (C) 120 min, and (D) close-up of the surface cracks developed after 120 min. Scale bar (A) 100 μm, (B and C) 20 μm, and (D) 2 μm.

cantilevers is about 20 μm smaller on the laser-ablated bottom than on the mirror side of the molding tool. The injection molding process parameters were melt temperature 200°C, tool temperature 40°C, and injection speed 9 cm^3 s^{-1}, i.e. similar to those used previously.[8,9]

Polymer Materials

Metallocene polypropylene (m-PP: Metocene HM 648T, LyondellBasell, Germany) was used as model polymer due to its pronounced shear thinning that favors filling of microcavities in injection molding applications. Other polymers used in the bioanalytical devices. such as cyclic olefin copolymer (COC: Topas 8007x10), polyoxymethylene (POM-C: 511P Delrin NC010), and polyvinylidenfluoride (PVDF: Kynar 720 Arkema) were also molded with the tool but not investigated in detail. However, because of the superior mold filling of PP and their subsequent application in sensing applications, the detailed investigation of the UVO exposure was conducted using the molded PP μCs only. Injection-molded PP μCs were stored at ambient conditions for at least 1 week before use to allow postcrystallization as the molded product's mechanical characteristics change substantially within the first 24 h after molding.[15]

Cantilever Finishing

Physical vapor deposition coating of cantilevers was carried out with a laboratory thermal evaporator (Balzers BAE 250, Balzers, Liechtenstein) employing evaporation material from Umicore (Cr and Au, both 99.99%). The layer thickness was controlled by means of a quartz crystal microbalance integrated in the evaporation system. PP μCs were first coated on the flat mirror side with a 4-nm thin chromium film as adhesion promoter for the subsequently deposited 20-nm thin gold layer, which guaranteed sufficient laser beam reflectivity for use in the Cantisens® research system (Concentris GmbH, Basel, Switzerland) for measuring deflection.

Cantilever Surface Cleaning

The flat mirror side of the cantilever surface was treated in a UVO cleaner (UV Clean Model 13550, Boekel Scientific, Feasterville PA). Batches of gold-coated and bare μCs were cleaned for periods ranging from 2 to 120 min. Cleaning experiments of other polymeric μCs (PVDF, POM, and COC) were also conducted.

Cantilever Characterization

Surface inspection was carried out by means of optical microscopy (DMRX, Leica Microsystems Jena GmbH, Germany) and scanning electron microscopy (SEM: Supra 55 VP, Carl Zeiss NTS GmbH, Oberkochen, Germany).

Reflection Fourier transform infrared (FTIR) spectra of two regions on the μC array, i.e. close to the cantilever fingers and holder, respectively, were recorded using a Centaurus IR-microscope coupled to a Nexus IR spectrometer (Thermo Electron, Thermo Fisher Scientific, Dreieich, Germany) with a grid of 300 μm × 300 μm. Two μC arrays of non-UVO-treated specimens were measured as reference. The background spectra were recorded every 15 min.

For the thermal analysis, the μC arrays with a mass between 3 and 4 mg were sealed to an aluminum cup to acquire

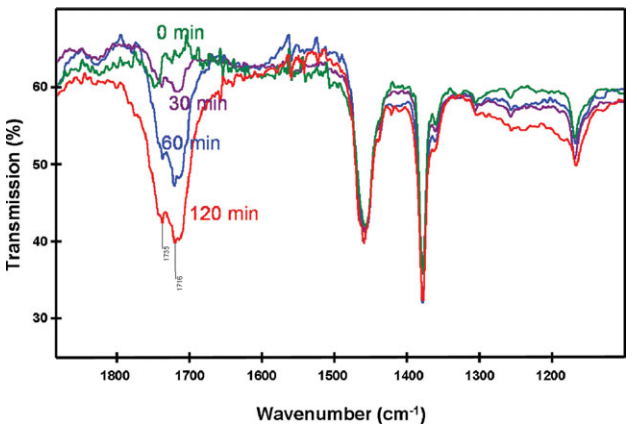

Figure 3. FTIR-Spectrum (reflection) of a PP μC in the region between 1850 and 1100 cm^{-1}. Two partially overlapping signals (1715 and 1735 cm^{-1}) show the formation of carbonyl and ester groups, their intensity correlating with the UVO exposure time. [Color figure can be viewed in the online issue, which is available at wileyonlinelibrary.com.]

differential scanning calorimeter (DSC: DSCQ1000, TA Instruments, Waters GmbH, Eschborn, Germany) data. The complete protocol, consisting of a first heating cycle from 0°C to 250°C, subsequent cooling to 0°C and a second heating cycle again to 250°C, was conducted in a dry nitrogen atmosphere. The heating and cooling rates were set to 10 K min^{-1}.

To evaluate the thermal behavior (bimetallic test), the gold-coated PP μCs were introduced into the water-filled cell of the Cantisens® research system maintained at 25°C. The temperature was increased at a rate of 0.2 K s^{-1} from 25°C to 30°C, and the bending response of each μC was recorded. The cantilevers bend because of the different thermal expansions of polymer and metal. The series of heat tests followed by an UVO exposure was conducted using three PP μC arrays from a single batch.

To determine the μC's hardness, the PP μCs were mounted on aluminum stubs by means of carbon tape for indentation tests. The hardness and elastic modulus of the μCs exposed to UVO were determined using a nanoindenter (MTS XP®, MTS Systems, Cary, NC) with a 1 μm conical tip (XP/CON100/001). For practical reasons, the indentation measurements were carried on the array holder and not on the μC itself. Indentations at two locations of each array were averaged. A maximum load of 5 mN was applied using a loading rate of 0.1 mN s^{-1}. The holding time was set to 30 s at maximum load, which allows the material to relax and clears the unloading data set from the creeping phenomena. The Poisson's ratio of PP corresponds to 0.4, as given by the supplier (see datasheet).

Bending tests were performed using a nanoindentation system (MTS XP®) operated under the load-control mode. A flat punch probe (XP/FLT 090/D0050) placed at the center of the UVO-treated PP μC was used to apply a load of 1 mN at maximum. The loading rate corresponded to 0.066 mN/s. The holding time was again set to 30 s.

RESULTS AND DISCUSSION

Materials Selection and μC Cross Section

Of the polymers tested, m-PP was most suitable for preparation of μCs as its pronounced shear thinning at relatively low temperatures enabled ready filling of the mold cavities. Figure 1 shows an SEM micrograph of injection-molded PP μCs. The μCs exhibit a trapezoid cross section [see Figure 1(B)], which reflects a relatively large draft angle compared with standard injection molding products. This draft angle facilitates demolding of the rather thin μC beams avoiding undesired plastic deformation.

Cantilever Characterization

The UVO cleaning procedure removes molecular levels of non-intentionally adsorbed organic species (contaminations) yielding a clean cantilever surface. Because the 20-nm thin gold coating does not present a major optical barrier for the UV light, the analysis is usually related to bare μCs. Mechanical degradation effects were expected to be equal or larger for the bare than for the gold-coated μCs.

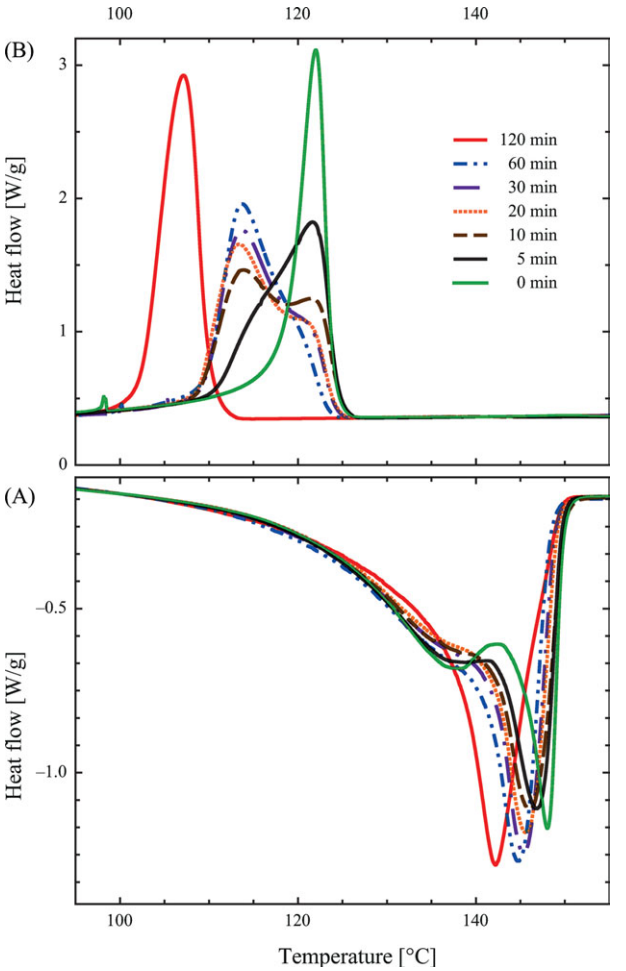

Figure 4. DSC measurement of PP μC arrays for different UVO exposure times displaying changes in the melting (A) and crystallization (B) behavior. [Color figure can be viewed in the online issue, which is available at wileyonlinelibrary.com.]

Table I. Summary of the Results From DSC Analysis of PP μCs Exposed to Different Doses of UVO

UV-ozone exposure (min)	0	2	5	10	15	20	30	60	120
1st heating									
T_{g1} (°C)	53	53	52	56	57	60	49	49	48
T_{m1} (°C)	146	146	146	146	146	146	147[a]	92/144	104/143
ΔH_{m1} (J/g)	72	76	78	78	78	75[b]	84	88	86
Cooling									
T_c (°C)	122	122	122	121/114	114[a]	113[a]	114	114	107
ΔH_c (J/g)	91	92	93	93	93	91[a]	92	94	89
2nd heating									
T_{m2} (°C)	139/148	138/148	139/147	145[a]	146[a]	146[a]	145	145	142
ΔH_{m2} (J/g)	93	95	95	94	94	93[b]	95	97	94

[a]Shoulder, [b]Actual numerical values of the enthalpies may be slightly higher than shown.

Figure 2, which is composed of SEM micrographs of a PP μC array after UVO treatment for different durations of exposure, shows significant morphological changes for exposure times above 30 min. For exposure times longer than 30 min, both optical microscopy and SEM [cp. images in Figure 2(B–D)] revealed crack-like microstructures on the μCs associated with surface etching, a phenomenon also present for the gold-coated μCs. This means that the coating does not prevent UVO etching of PP μCs for exposure times above 30 min.

SEM data show that the surface roughness increases with exposure time, as observed for oxygen plasma treatments.[16] Two kinds of surface patterns were distinguishable, one of flow lines and the other of microcracks. Flow lines correspond to surface textures or voids owing to local filling inhomogenities along the flow direction. The microcracks are formed almost perpendicular to the μC direction illustrating flow instabilities caused during filling of the micrometer-thin mold cavity. The microcracks, which are discontinuous along the μC, are first formed at the base of the μCs. With increasing UVO exposure time, they evolve like bands along the entire μC. The microcracks are almost straight at the base of the μC and later follow the polymer flow direction along the length of the μC. They seem to be the result of polymer shrinkage in the beam direction. This may arise from the nonlinear flow front owing to the lower viscosity at the sidewalls of the mold.

On UVO exposure the polymer degrades. This means that due to the transparency of PP to UV light, low molecular weight fragments are formed through chain scission in the entire holder, resulting in a reduced glass transition temperature T_g.[17,18] They undergo oxidative reactions, once cracks are formed at the surface. Callen et al.[19] demonstrated that UVO treatments of PS produces oxidized polymer surfaces comprising of C—O, C=O, and O—C=O groups.

The FTIR spectra of the UVO-exposed PP μCs, as shown in Figure 3, feature two carbonyl signals at the wavelengths of 1734 cm^{-1} (ester) and 1716 cm^{-1} (ketone or unsaturated ester), indicating thermo-oxidative aging. Comparing the spectra for the selected exposure times, a detection threshold for the carbonyl bands of about 20 min can be identified. For longer exposure times, the carbonyl-related peak intensities correlated well with the duration of the UVO treatment. Carboxylic acids and free OH groups are present at wavelengths of about 3400 cm^{-1} (intermolecular OH bonds; not shown in Figure 3). These signals became stronger for exposure times of 60 and 120 min.

Complementary information regarding the underlying physical and chemical phenomena was gained through thermal analysis by means of DSC. For this purpose μCs with UVO treatments were subjected to heating and cooling cycles. Figure 4 and Table I summarize the transition temperatures and enthalpies. Increasing the exposure time, the transition temperatures shifted to smaller values. The degree of crystallinity, characterized by means of ΔH_{m1}, increases with the exposure time. An UVO exposure less than 30 min leads to an increase in crystallinity of 5–10%, whereas an exposure of 30 min and longer increases the crystallinity up to 25%. Such significant changes in crystallinity are characteristic for physical aging in semicrystalline polymers.[20] The cooling reveals that the recrystallization is shifted

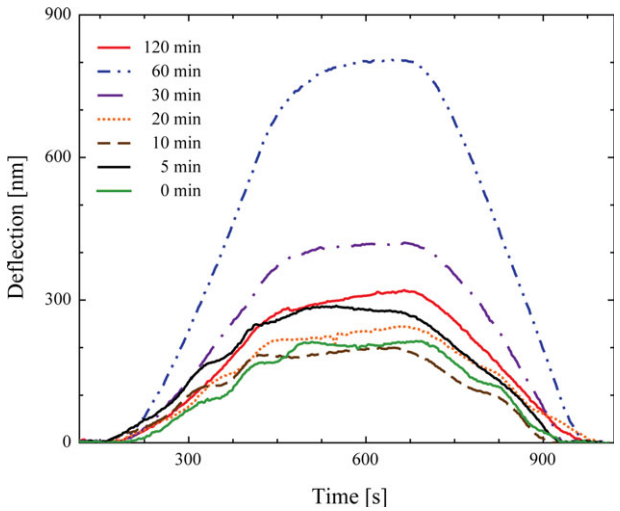

Figure 5. Deflection due to the bimetallic effect of the gold-coated PP μC #5 for the different UVO exposure times. [Color figure can be viewed in the online issue, which is available at wileyonlinelibrary.com.]

Applied Polymer SCIENCE

Table II. Maximum Deflection Recorded During the Heat Test of the Gold-Coated UVO-Exposed PP μCs (Results Averaged for All eight μCs From three Samples)

UV-ozone exposure (min)	0	2	5	10	15	20	30	60	120
Deflection (nm)									
μC array 1	270 ± 139	264 ± 110	292 ± 122	168 ± 130	213 ± 92	344 ± 153	686 ± 175	602 ± 347	483 ± 120
μC array 2	196 ± 91	298 ± 98	249 ± 80	279 ± 133	202 ± 73	208 ± 80	384 ± 182	526 ± 77	288 ± 147
μC array 3	267 ± 187	374 ± 174	273 ± 190	428 ± 254	295 ± 164	383 ± 218	458 ± 179	446 ± 196	352 ± 168

Table III. Deformation Characteristics of the Surface of the UVO Exposed PP μC Array Holders as Determined From Indentation Experiments

UV-ozone exposure (min)	0	2	5	10	15	20	30	60	120
Modulus (MPa)	887 ± 18	783 ± 28	632 ± 17	242 ± 60	808 ± 37	1060 ± 70	1001 ± 2	1314 ± 67	1467 ± 28
Hardness (MPa)	21 ± 0.42	17 ± 1	16 ± 0.32	1 ± 0.2	19 ± 1	26 ± 1	20 ±1	22 ± 0.44	18 ± 0.36

toward smaller transition temperatures, an effect already detected for exposure times as small as 5 min. The related enthalpy ΔH_c, however, is unaffected for exposures up to 20 min. This behavior indicates the onset of *cross linking*. A decreasing melting temperature (T_m) with increasing exposure time is observed for the second heating cycle shown in Figure 4. This effect is attributed to *chemical aging* initiated already after an UVO exposure of 5 min. Additionally, the appearance of a secondary peak at the temperature T_{m1} during the melting process is only observed for exposure times of 30, 60, and 120 min. The glass transition temperature T_g amounts to 56 ± 4°C for UVO exposures up to 20 min (see Table I). Longer exposures result in a drop by about 10 K.

The mechanical behavior of gold-coated, UVO-treated μCs was characterized taking advantage of the thermally induced bending of the biphasic cantilever, often referred to as heat test.[21] Due to the difference in the linear coefficient of thermal expansion (α) of the 24-nm thin metal ($\alpha_{gold} = 14.2 \times 10^{-6}$ K^{-1}) and the 35-μm thick PP ($\alpha_{PP} = 150 \times 10^{-6}$ K^{-1}), the μC bends, which is detected through laser beam deflection at the μC free end. Figure 5 shows deflection curves of selected PP μCs after UVO treatment. For exposure times up to 20 min, the curves illustrate some variations but are comparable to the base line (no UVO treatment). The increase in the deflection signal for 30 and 60 min exposures coincidences with the observation of crack-like surface microstructures in optical microscopy. The variation in the mean deflection values as given in Table II, demonstrates that the deflection can massively change from array to array. The main result, a step-like increase in the deflection signal between 20 and 30 min of exposure time, leads to the conclusion that the μCs can be UVO treated for up to 20 min.

Nanoindentation usually provides mechanical data of a combination of surface and bulk properties and might, thus, be more appropriate to characterize the UVO-induced modifications of the

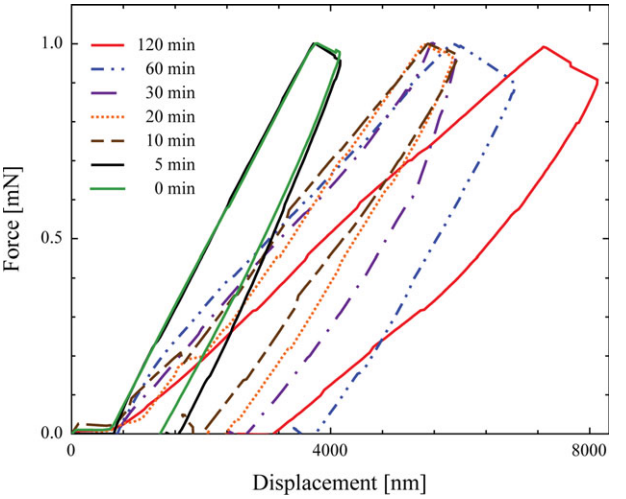

Figure 6. Load–deflection curves from the bending of the PP μC using the nanoindenter. The Young's modulus of the PP μC was obtained from the slope of the load–deflection curve (cf. Table IV). [Color figure can be viewed in the online issue, which is available at wileyonlinelibrary.com.]

Table IV. Deformation Characteristics of UVO-Exposed PP μCs as Determined From Bending Experiments

UV-ozone exposure (min)	0	2	5	10	15	20	30	60	120
Modulus (GPa) (eq. (1))	3.16 ± 0.44	2.78 ± 0.83	3.07 ± 0.64	2.07 ± 0.96	2.16 ± 0.94	2.71 ± 0.39	2.76 ± 0.15	1.62 ± 0.39	1.40 ± 0.35
Stiffness (N/m)	241 ± 26	216 ± 65	209 ± 65	161 ± 75	168 ± 17	210 ± 29	214 ± 38	126 ± 29	108 ± 27

μCs. Such a measurement does not only allow for determination of the local hardness but also of the Young's modulus from the slope of the unloading curve.[22] Table III summarizes these two quantities, including their error bars as a function of exposure time. After a decrease during the first 10 min of exposure, the Young's modulus increases with exposure time but a pronounced, distinct change between 20 and 30 min UVO treatments cannot be found. On the contrary, the hardness shows a maximum for 20 min exposure. Nevertheless we assume that the hardness is largely insensitive to UVO treatments, which may arise from the fact that not the cantilevers themselves but the rather bulky connection part of the cantilever array was tested, where no or few cracks are formed at extended UVO exposure times.

Figure 6 displays load–displacement curves (P–z) of PP μC as a function of UVO exposure time. The elastic modulus of the μC can be derived using the equation:

$$E = \frac{4L_e^3}{wt^3}\left(\frac{P}{z}\right) \quad (1)$$

where w and t denote the μC width and thickness, respectively. L_e is the equivalent beam length between the loading position and the fixed end of the μC. The parameter (P/z) is the stiffness of the μC associated with the length L_e, and is given by the slope of the load–displacement curve. Table IV summarizes the mean values, including error bars. For UVO exposure times of up to 30 min, both Young's modulus and stiffness remain constant. Both experimental values significantly decline for UVO treatments above 30 min. Therefore, we conclude from the bending measurements that exposure times larger than 30 min have to be avoided to maintain the desired bending characteristics.

CONCLUSIONS

UVO treatment can significantly influence the physical and chemical properties of PP μCs. A reasonable compromise between the negative impact on the latter and the cleaning efficacy was found for UVO exposure times up to 20 min. Longer UVO treatments cannot be tolerated as severe deterioration of the bending and surface characteristics takes place. Nanometer-thin gold coatings, often deposited to obtain reasonable laser beam reflectivity, do not prevent the μC degradation but cause a moderate retardation of the UVO-induced property modification.

ACKNOWLEDGMENTS

This research was funded by the Swiss Nanoscience Institute (SNI) through the applied research project DICANS, a collaborative initiative between the Biomaterials Science Center (BMC) of the University of Basel, the Paul Scherrer Institut (PSI), the University of Applied Sciences Northwestern Switzerland (FHNW) and Concentris GmbH. The authors thank K. Jefimovs (EMPA Dübendorf) for the laser micromachining of the mold, O. Häfeli and E. Kramer (FHNW Windisch) for the injection molding and polymer analysis, R. Ghisleni (EMPA Thun) for his assistance with the MTS XP® system, M. Altana and C. Spreu from PSI for their technical assistance.

REFERENCES

1. Greiner bio-one. Chemical-and-thermal-resistance-of-polypropylene–polystyrene–LDPE–HDPE–EVA and UV-Star. http://www.biocompare.com/Articles/ApplicationNote/1609/
2. Giboz, J.; Copponnex, T.; Mélé, P. *J. Micromech. Microeng.* **2007,** *17*, 96–109.
3. Heckele, M.; Schomburg, W. K. *J. Micromech. Microeng.* **2004,** *14*, R1–R14.
4. Berger, R.; Gerber, C.; Lang, H. P.; Gimzewski, J. K. *Microelectron. Eng.* **1997,** *35*, 373–379.
5. Genolet, G.; Despont, M.; Vettiger, P.; Anselmetti, D. *J. Vac. Sci. Technol. B* **2000,** *18*, 617–620.
6. Nordström, M.; Keller, S.; Lillemose, M.; Johansson, A.; Dohn, S.; Haefliger, D.; Blagoi, S.; Havsteen-Jakobsen, S.; Boisen, A. *Sensors* **2008,** *8*, 1595–1612.
7. McFarland, A.; Poggi, M. A.; Bottomley, L. A.; Colton, J. S. *Nanotechnology* **2004,** *15*, 1628–1632.
8. Urwyler, P.; Schift, H.; Gobrecht, J.; Häfeli, O.; Altana, M.; Battiston, F.; Müller, B. *Sens. Actuators A: Phys.* **2011,** *172*, 2–8.
9. Urwyler, P.; Häfeli, O.; Schift, H.; Gobrecht, J.; Battiston, F.; Müller, B. *Procedia Eng.* **2010,** *5*, 347–350.
10. Vig, J. R. *J. Vac. Sci. Technol. A* **1985,** *3*, 1027–1034.
11. Köser, J.; Gaiser, S.; Müller, B. *Eur. Cells Mater.* **2011,** *21*, 479–487.
12. Wypyh, G. Handbook of Material Weathering; ChemTec Publishing: Toronto, **2003.**
13. Bhattacharyya, A.; Klapperich, C. *Lab Chip* **2007,** *7*, 876–882.
14. Zhou, Q.; Xanthos, M. *Polym. Degrad. Stabil.* **2009,** *94*, 327–338.
15. Kristiansen, M.; Tervoot, T.; Smith, P.; Goosens, J. P. G. *Macromolecules* **2005,** *38*, 10461–10465.
16. Tsougeni, K.; Vourdas, N.; Tserepi, A.; Gogolides, E.; Cardinaud, C. *Langmuir* **2009,** *25*, 11748–11759.
17. Nie, H.-Y.; Walzak, M. J.; Berno, B.; McIntrye, N. S. *Appl. Surf. Sci.* **1999,**144–145,627–632.
18. Eve, S.; Mohr, J. *Procedia Eng.* **2009,** *1*, 237–240.
19. Callen, B. W.; Ridge, M. L.; Lahooti, S.; Neumann, A. W.; Sodhi, R. N. S. *J. Vac. Sci. Technol. B* **1995,** *13*, 2023–2029.
20. Msuya, W. F.; Yue, C. Y. *J. Mater. Sci. Lett.* **1989,** *8*, 1266–1268.
21. Urwyler, P.; Köser, J.; Schift, H.; Gobrecht, J.; Müller, B. *Biointerphases* **2012,** *7*, 8.
22. Cheng, C.-M.; Cheng, Y.-T. *Appl. Phys. Lett.* **1997,** *71*, 2623–2625.

AIP | Journal of Applied Physics

Nanometer-size anisotropy of injection-molded polymer micro-cantilever arrays

Prabitha Urwyler, Hans Deyhle, Oliver Bunk, Per Magnus Kristiansen, and Bert Müller

Citation: J. Appl. Phys. **111**, 103530 (2012); doi: 10.1063/1.4720942
View online: http://dx.doi.org/10.1063/1.4720942
View Table of Contents: http://jap.aip.org/resource/1/JAPIAU/v111/i10
Published by the American Institute of Physics.

JOURNAL OF APPLIED PHYSICS **111**, 103530 (2012)

Nanometer-size anisotropy of injection-molded polymer micro-cantilever arrays

Prabitha Urwyler,[1,2] Hans Deyhle,[1,3] Oliver Bunk,[3] Per Magnus Kristiansen,[4] and Bert Müller[1,a)]
[1]*Biomaterials Science Center, University of Basel, c/o University Hospital, 4031 Basel, Switzerland*
[2]*Laboratory for Micro- and Nanotechnology, Paul Scherrer Institute, 5232 Villigen PSI, Switzerland*
[3]*Swiss Light Source, Paul Scherrer Institute, 5232 Villigen PSI, Switzerland*
[4]*Institute of Polymer Engineering (IKT) and Institute of Polymer Nanotechnology (INKA), School of Engineering, University of Applied Sciences and Arts Northwestern Switzerland, 5210 Windisch, Switzerland*

(Received 5 January 2012; accepted 23 April 2012; published online 30 May 2012)

Understanding and controlling the structural anisotropies of injection-molded polymers is vital for designing products such as cantilever-based sensors. Such micro-cantilevers are considered as cost-effective alternatives to single-crystalline silicon-based sensors. In order to achieve similar sensing characteristics, structure and morphology have to be controlled by means of processing parameters including mold temperature and injection speed. Synchrotron radiation-based scanning small- (SAXS) and wide-angle x-ray scattering techniques were used to quantify crystallinity and anisotropy in polymer micro-cantilevers with micrometer resolution in real space. SAXS measurements confirmed the lamellar nature of the injection-molded semi-crystalline micro-cantilevers. The homogenous cantilever material exhibits a lamellar periodicity increasing with mold temperature but not with injection speed. We demonstrate that micro-cantilevers made of semi-crystalline polymers such as polyvinylidenefluoride, polyoxymethylene, and polypropylene show the expected strong degree of anisotropy along the injection direction. © *2012 American Institute of Physics*. [http://dx.doi.org/10.1063/1.4720942]

I. INTRODUCTION

Injection-molded polymer parts exhibit a *skin-core* morphology and the related mechanical properties. They naturally show a relatively sharp transition between the homogeneous core with spherulite crystallites and the inhomogeneous skin composed of oriented and elongated crystallites, referred to as the shish-kebab structure.[1]

The injected polymer melt cools down at the mold wall within milliseconds via the heat conducting metal (Fig. 1), which leads to the formation of an oriented but amorphous skin layer, here termed Zone A.[2] Adjacent to this skin layer, the highly oriented transient layer, termed Zone B, forms. Since Zone A acts as a heat flow barrier, partial crystallization in Zone B takes place. As the heat transfer from the polymer toward the mold becomes less and less efficient, the intermediate shear layer, Zone C, develops. It is distinguished by the partial relaxation of shear-induced orientations before solidification.[1–4] After cessation of the polymer flow, the cooling rate in the core, termed Zone D, is so low that only spherulitic superstructures[2] with relaxed chains are established. The thickness of the four zones strongly depends on the processing and can also be manipulated incorporating nucleating agents.[5,6] The mold temperature affects the solidification of the selected polymer.[7] The fraction of the skin layer markedly increases with melt temperature, while the fraction of the shear zone varies with the injection pressure.[8]

The *skin-core* morphology not only depends on the process parameters but also on the shape and size of the polymer products. It has been pointed out that higher molecular orientation occurs with decreasing cavity thickness.[9] Therefore, we expect to locate highly ordered polymer molecules in injection-molded micro-cantilevers.

The correlation between structure and function is known from the literature.[5] The mechanical properties of the injection-molded polymer products significantly derive from the highly oriented skin layers formed through shear-induced crystallization.[5] The skin layer may become dominant in microstructures. For micro-cantilevers (μC), the skin might even fill the entire cross-section, so that the isotropic core is absent. Therefore, the bending characteristics of μCs may crucially depend on the selected process parameters including mold temperature and injection pressure.

The understanding of the μC properties requires detailed analysis of their structure including anisotropy. The present communication concentrates on spatially resolved small- and wide-angle synchrotron x-ray scattering (SAXS and WAXS) as these methods cover the entire nanometer range.[10] Both techniques were already used to reveal a gradual change of molecular orientation from the periphery to the center of injection-molded specimens.[11,12]

It should be noted that amorphous and semi-crystalline polymers have been used for injection molding of polymeric micro-cantilevers.[13] Amorphous polymers show homogeneous arrangement of molecules and a lack of short- and long-range orders. Semi-crystalline polymers generally exhibit ordering on molecular and supra-molecular levels. The semi-

a)E-mail: bert.mueller@unibas.ch. Tel.: +41 (0)61 265 96 60. Fax: +41 (0)61 265 96 99.

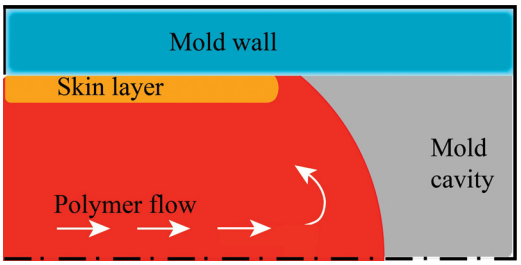

FIG. 1. Mold filling involves flow of polymer melts and solidification of the melt starting at the walls. Fountain flow describes how the polymer fills the mold cavity. Molecules from the center of the cavity flow towards the wall and form a stable skin layer. This causes a higher degree of molecular orientation in the skin layer compared to bulk.

crystalline polymers represent a characteristic lamellar morphology of stacks composed of crystalline and amorphous regions. These stacks contain crystals of distinctive thickness (l_c) and amorphous layers of thickness l_a in between. These lengths define the long period as $L = l_c + l_a$ which is in the order of 10 nm and depends on the selected polymer.[14]

II. EXPERIMENTAL

A. Injection molding

A laser-machined mold insert was used for the fabrication of arrays of 8 μC, featuring cavities of 480 μm × 100 μm × 45 μm. The first generation of the mold insert (Steel 1.2312) was micro machined using a ns-laser (YAG, Coeheret Avia, wavelength 355 nm, pulse duration 20 ns). The second-generation mold insert incorporated high-quality steel with small grain size (Polmax Uddeholm) and was micro machined using a ps-laser ablation system (YAG-laser, SuperRapid, Lumera, 355 nm, pulse duration 10 ps). The small grain size of the mold material along with ps-laser ablation resulted in sharp edges, better accuracy, and less roughness. Injection-molding experiments were performed on an Arburg 320 ALLROUNDER (Arburg, Lossburg, Germany).

The following polymer materials were injection molded at the given temperatures of melt T_{melt}, polyetheretherketone (PEEK: AvaSpire AV-650 BG15, Solvay Advanced Polymers GmbH, Düsseldorf, Germany, $T_{melt} = 400\,^{\circ}C$), polypropylene (PP: Metocene HM 648 T, LyondellBasell, Bayreuth, Germany, $T_{melt} = 200\,^{\circ}C$), polyoxymethylene copolymer (POM: 511 P Delrin NC010, $T_{melt} = 220\,^{\circ}C$), cyclic olefin copolymer (COC: Topas 8007 X 10, TOPAS Advanced Polymers GmbH, Frankfurt-Höchst, Germany, $T_{melt} = 240\,^{\circ}C$), and polyvinylidenefluoride (PVDF: Kynar 720, Arkema Puteaux, France, $T_{melt} = 220\,^{\circ}C$). Details on the commercial polymer grades used as well as supplementary information on the processing are published.[13] For this study, the polymer μC were injection molded at the two following mold temperatures (T_{mold}) keeping the injection speed at 9 cm^3/s (PP: 40 °C, 80 °C; PVDF: 80 °C, 120 °C; POM: 120 °C, 150 °C). The dependence of the structure on injection speed for PP 5, 10, and 20 cm^3/s; for PVDF 10 and 20 cm^3/s; and for POM 10 and 20 cm^3/s was studied as well.

The micro-cantilevers were produced in batches of 20 arrays. One array per batch was investigated using x-ray scattering.

B. X-ray scattering

The 8 μC of each individual array were examined using scanning SAXS and WAXS. SAXS and WAXS patterns of the injection-molded micro-cantilever arrays were obtained at the cSAXS beamline at the Swiss Light Source, Villigen, Switzerland,[10] at a photon energy of 11.2 keV (wavelength 1.107 Å). SAXS data were acquired within three distinct beamtimes. The x-ray beam was focused to about 25 μm × 5 μm, 30 μm × 30 μm, and 25 μm × 5 μm in horizontal and vertical directions, respectively. Silver behenate powder diffraction served to determine the sample-detector distance of 7.1 m for SAXS and 0.4 m for WAXS measurements.

The micro-cantilever arrays were mounted on a frame and translated perpendicular to the beam by means of a motorized 2D manipulator. Diffraction patterns were recorded on a 2D PILATUS detector with a pixel size of 172 μm.[10] The exposure time was 2 s for WAXS and 0.150 s for SAXS. For WAXS, the specimens were mounted with the cantilevers oriented vertically. For SAXS, the specimens were mounted with the cantilevers oriented horizontally to study the cantilever rim region with highest possible resolution. The scanning was performed line wise: the specimens were moved in the horizontal direction through the beam at constant speed while the x-ray detector recorded data continuously. The covered length on the specimen for each frame corresponded to 20, 25, and 15 μm, respectively, while the distance between the lines corresponded to 10, 20, and 15 μm. The air scattering was collected for a sample-free area and was subtracted from each frame. Data treatment was performed using self-written MATLAB 7.6.0 (The MathWorks, Inc., MA, USA) code.[10]

The arrays for the temperature-dependent study were measured within two beamtimes with step sizes of 20 μm × 10 μm and 20 μm × 25 μm. This means, 48 μC per material were examined. The arrays for the speed-dependent study were examined during another beamtime with a step size of 15 μm × 15 μm. Here, 48 μC for PP, 24 μC for PVDF, and 24 μC for POM were included into the study.

III. RESULTS AND DISCUSSION

A. Injection molding

Fig. 2 shows images of injection-molded polymeric μC using two generations of molds. The improved mold fabrication led to a much better shape of the μC (cf. images in the first and the second row in Fig. 2). The polymers PP, POM, and PVDF completely filled the mold cavities in spite of the high-aspect ratio of the microstructure (cf. images for PP in Fig. 2). PEEK, which requires mold temperatures above 320 °C, only partially filled the mold. For the COC μC, successful de-molding was usually impossible owing to its inherent brittleness.

The two optical micrographs on the left side of Fig. 2 display dark rim-like regions at the edges of each μC. These rim-like regions might be the result of slant edges causing refraction.

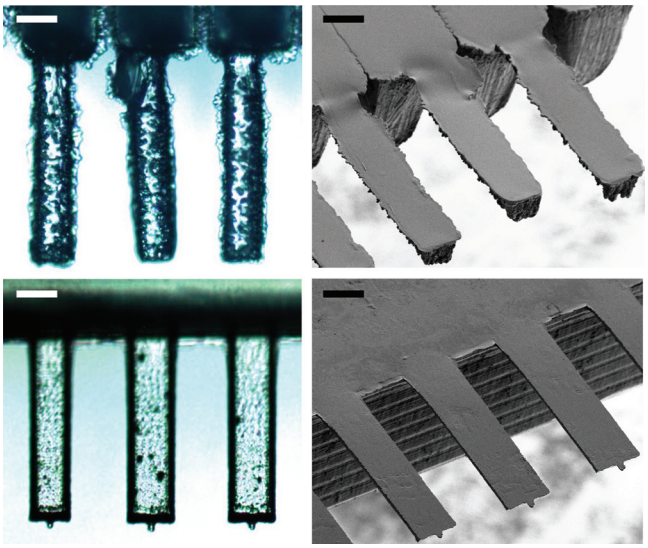

FIG. 2. Optical and SEM micrographs of injection-molded PP μC (mold temperature 80 °C). The scale bars correspond to 100 μm. The images of the first and second rows demonstrate the development from the first- to the second-generation injection molds. The optical micrographs show rim-like regions at the edges of the μC.

B. Wide-angle x-ray scattering

WAXS supports the identification of crystalline phases, the degree of crystallinity, and the average orientation of molecules. Crystalline materials give rise to diffraction patterns with spots and/or sharp rings, whereas amorphous materials only produce broad, diffuse rings characteristic for the short-range order.

Fig. 3 represents 2D WAXS patterns of the four polymers COC, PEEK, POM, and PP measured at the rim regions and the center of the μC. The patterns from rim and center only differ in intensity. This difference results from the μC's thicknesses, which is smaller at the μC rim. Note that the two distinctive spots present in all images of Fig. 3 are artifacts, i.e., diffraction from the x-ray beam exit window made of mica muscovite, a single crystalline mineral.

WAXS patterns from COC and PEEK μC exhibit a halo, which is characteristic for amorphous materials without preferred orientation. For COC, the co-polymerization of ethylene with norbornene renders the structure amorphous. PEEK, which is generally found in a semi-crystalline state, was found to be amorphous. We assume that this is due to the fast cooling rate during μC fabrication.

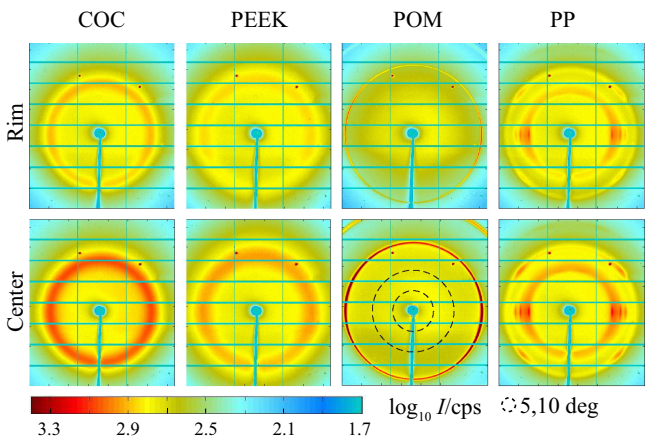

FIG. 3. Wide-angle x-ray scattering patterns of the first generation μC measured at the rim (top row) and center (bottom row). The WAXS patterns from rim and center only differ in intensity.

The WAXS patterns of POM and PP show features characteristic for semi-crystalline structures with moderate (POM) or even quite distinct (PP) average orientation of molecules. For POM, a sharp ring at $q = 16.21\,\mathrm{nm}^{-1}$ is present, which corresponds to a spacing of $d = 0.38$ nm. Note that the two dashed circles represent scattering angles of 5° and 10°, respectively. The radial integration of the WAXS patterns from PP reveals the presence of the distinct peaks at q-values of 15.45, 13.16, 12.02, 10.66, and 10.12 nm^{-1}. The related d-values, i.e., 0.40, 0.47, 0.52, 0.58, and 0.62 nm, correspond to the α and β phases of PP.

C. Small angle x-ray scattering

The optical micrographs of Fig. 2 show a rim region around each μC, which is also visible in the spatially resolved SAXS patterns (see inset of Fig. 4). The color-coded SAXS data of the inset illustrate the preferential orientation of the scattering, which is found to be perpendicular to the μC near the edges (cf. color wheel in Fig. 4). The integral scattered intensity across individual COC, PP, POM, and PEEK μC reveals strong edge signals, which are much stronger, compared to the signal from the μC's center and can be fitted by means of Gaussians. The full-width-at-half-maximum (FWHM) of the Gaussians does not depend on the selected polymer and amounts to (21.8 ± 0.5) μm. From our point of view, it is implausible that this width, constant for the four selected polymer materials, relates to the skin layer thickness. Therefore, we assume that the presence of these strong edge signals arises from edge scattering of the elliptically shaped x-ray beam within the sloped region of the

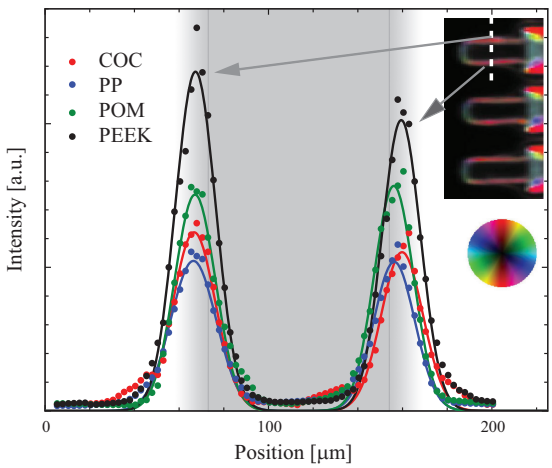

FIG. 4. SAXS intensity distribution (286–418 nm) integrated along the first generation μC. High scattering intensities are present at the rim-like regions for COC, PP, POM, and PEEK. The constant full-width-at-half-maximum of (21.8 ± 0.5) μm is attributed to edge scattering and characterizes the x-ray beam width. The edge scattering even shows a preferential orientation as indicated by the inset. The orientation is color-coded according to the color wheel inset. The gray area indicates the width of the cantilever, while the gradient of the gray color indicates the thickness.

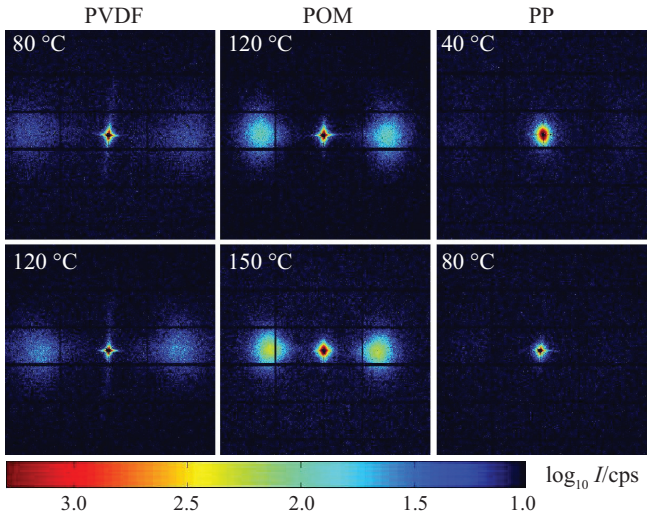

FIG. 5. The SAXS pattern at the center of PVDF, POM, and PP second-generation μC exhibit characteristic features, which become closer for higher mold temperatures. This means the observed nanostructures increase with the mold temperature.

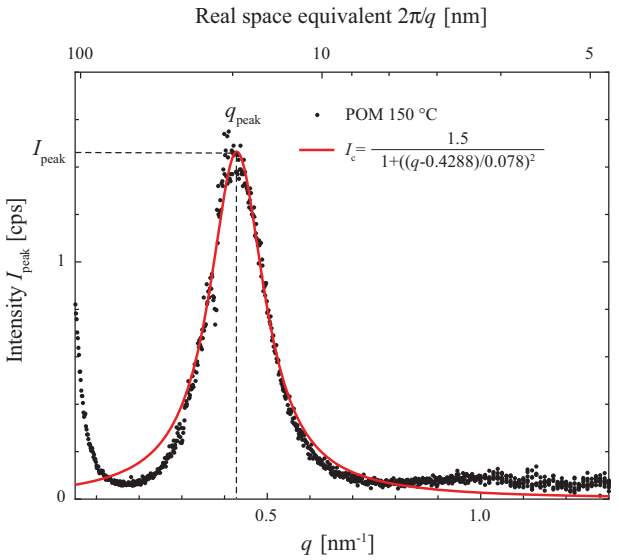

FIG. 6. The spots of the SAXS pattern shown in Fig. 5 are quantified using the peak intensity I_{peak}, the q-value at the peak q_{peak}, and the full-width-at-half-maximum $FWHM_{peak}$ of the spot derived from a fit to a Lorentzian (cf. Table I). The graph shows this procedure exemplarily for POM using the mold temperature of 150 °C.

cantilever rim. The thickness of the skin layer is expected to be in the same range or even smaller than the beam width and thus cannot be determined with this direct scanning SAXS approach, because the observed scattering effect overshadows the skin region.

In order to demonstrate the anisotropy of the μC, SAXS patterns acquired within the center of the cantilevers were examined. Fig. 5 contains such background-corrected patterns for PVDF, POM, and PP μC fabricated using the mold temperatures indicated. Besides the central SAXS pattern around the direct-beam stop, one finds two diffraction spots in flow (horizontal) direction, which are more prominent for POM than for PVDF and PP. For PP, these spots are hardly visible, indicating low degree of crystallinity. The distance of the spots from the beam stop is material dependent and decreases with the mold temperature. This means that by increasing the mold temperature, larger nanostructures are formed.

We believe that the related periodicities are crystalline lamellae in the injection-molded polymers. The repeat spacing of the crystalline lamellae of semi-crystalline polymers produces these long-period SAXS patterns. The radial integration of the scattering patterns allows characterization of the lamellar periodicity through extraction of three empirical parameters, i.e., peak intensity I_{peak}, peak position q_{peak}, and the full-width-at-half-maximum $FWHM_{peak}$ by fitting the peaks with a Lorentzian (cf. Fig. 6). Before fitting, the q-plots were background corrected with a correction function $I_{corr} \sim q^{-n}$. The correction exponent n was chosen such that the baseline of the investigated peak was flat (cf. Fig. 6). The related n was different for PVDF, POM, and PP and depended on the selected mold temperatures. The derived values of n are compiled in Table I. After this background correction, the peaks in the q-plots can be reasonably fitted using a Lorentzian as the red-colored curve exemplarily demonstrates for a POM μC fabricated with a mold temperature of 150 °C. Table I lists the fitted parameters for PVDF, POM, and PP at the selected mold temperatures. The decrease of q_{peak} with mold temperature is the most striking feature. The higher mold temperature results in larger lamellar crystals.

Fig. 7 shows the variation of I_{peak}, q_{peak}, and the $FWHM_{peak}$ across selected representative cantilevers. In the central part (constant thickness, cf. cantilever width given in gray), I_{peak} forms a plateau with approximately constant height. It decreases with reducing cantilever thickness (cf. gradient in gray color). The $FWHM_{peak}$ and q_{peak} show only negligible variations even when the μC-thickness diminishes. The

TABLE I. Nanostructure characterization of micro-cantilevers injection-molded at different mold temperatures. Mean values and related standard deviations of the three Lorentzian fitted values and the degree of anisotropy of the central region of the cantilever.

Material	PVDF		POM		PP	
Mold temperature (°C)	80	120	120	150	40	80
I_{peak} (counts per second)	0.409 ± 0.002	0.776 ± 0.046	1.740 ± 0.008	1.478 ± 0.014	0.0568 ± 0.0004	0.353 ± 0.005
q_{peak} (nm^{-1})	0.6439 ± 0.0010	0.5591 ± 0.0006	0.5066 ± 0.0005	0.4287 ± 0.0007	0.6674 ± 0.0027	0.5485 ± 0.0156
$FWHM_{peak}$(nm^{-1})	0.1991 ± 0.0028	0.1502 ± 0.0013	0.1013 ± 0.0010	0.0785 ± 0.0015	0.2203 ± 0.0110	0.2743 ± 0.0389
Correction exponent (n)	0.90	0.82	0.75	0.95	0.75	0.45
Degree of anisotropy	0.717 ± 0.005	0.893 ± 0.001	0.953 ± 0.002	0.940 ± 0.001	0.440 ± 0.019	0.207 ± 0.009

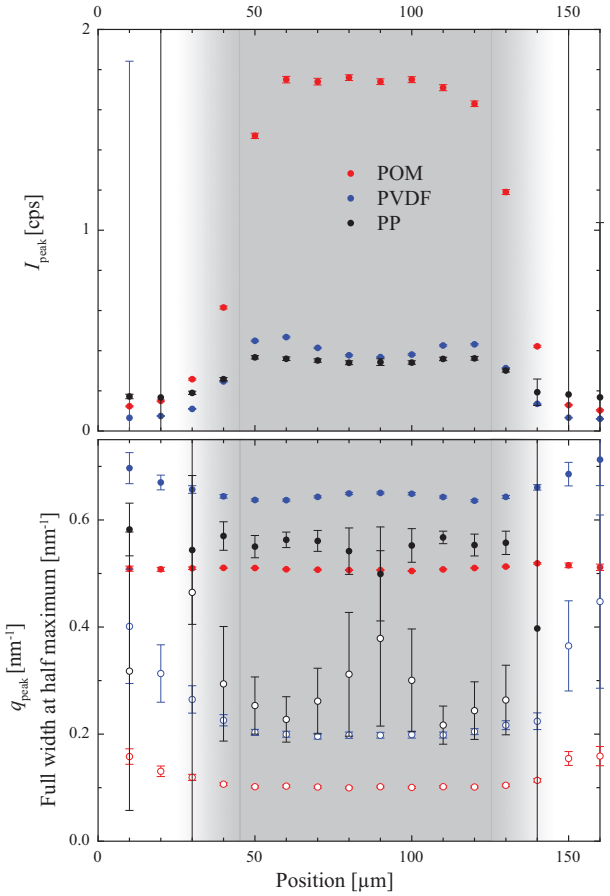

FIG. 7. The spatially resolved SAXS pattern (16 points across the width of the second-generation μC) demonstrates the homogeneity of the POM, PVDF, and PP μC using the three fitted parameters (cf. Fig. 6).

relatively low scattering intensity for PP leads to large error bars. The low intensity variations in the central part of the μC indicate a homogeneous semi-crystalline structure.

The anisotropy of the μC related to the superstructures discussed above can be derived from the azimuthal intensity distribution. Fig. 8 displays such a plot for a POM μC fabricated at the mold temperature of 150 °C. The diagram contains the mean scattered intensity in the q-range between 0.35 and 0.51 nm^{-1} values, averaged over six frames of 0.150 s exposure time each, as a function of the azimuthal angular position. The error bars correspond to the standard deviation between the frames. The air scattering signal was subtracted from each frame. The opposing segments were

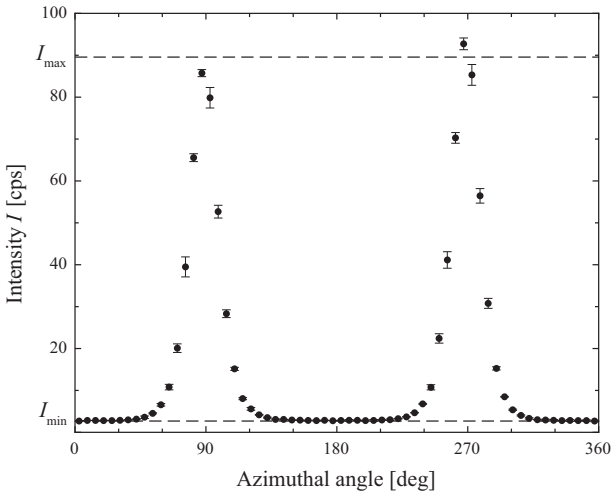

FIG. 8. The azimuthal plot (q-range of 0.35–0.51 nm^{-1}) of the mean scattered intensity of second-generation POM μC injection molded with a mold temperature 150 °C elucidates the orientation of the related nanostructures. The degree of orientation is determined by means of I_{max} and I_{min}.

averaged to gain the minimal and maximal intensities, I_{min} and I_{max} (cf. dashed lines in Fig. 8). The degree of anisotropy is defined as $(I_{max} - I_{min})/(I_{max} + I_{min})$. A strong orientation of the semi-crystalline lamellae stacks within the μC is observed for the three semi-crystalline polymers. The degree of anisotropy increases with mold temperature as summarized in Table I. Higher mold temperatures prevent early freezing. Therefore, the development of larger and well-oriented nanostructures is enhanced. There is, however, no significant dependence on the injection speed as verified by the data shown in Table II. Both the degree of anisotropy and the q_{peak}-values of the three semi-crystalline polymers do not change for the different injection speeds.

IV. CONCLUSIONS

Synchrotron radiation-based x-ray scattering provides a wealth of information to quantitatively characterize injection-molded polymer microstructures. Contrary to the established *skin-core* morphology models with zones of different crystallinity,[8,15] the spatially resolved SAXS and WAXS data elucidate that the μCs are homogeneous in the scanning directions perpendicular to the beam. Their crystalline structure, however, exhibits a strong anisotropy. Both crystallinity and anisotropy can be controlled by changing the mold temperature but not the injection speed.

TABLE II. Nanostructure characterization of micro-cantilevers injection-molded with different injection speeds. Mean values and related standard deviations of the three Lorentzian fitted values and the degree of anisotropy of the central region of the cantilever.

Material	PVDF		POM		PP		
Injection speed (cm^3/s)	10	20	10	20	5	10	20
I_{peak} (counts per second)	2.000 ± 0.0004	0.218 ± 0.0004	2.846 ± 0.0144	1.474 ± 0.0036	0.163 ± 0.0008	0.168 ± 0.0008	0.155 ± 0.0008
q_{peak} (nm^{-1})	0.562 ± 0.0005	0.558 ± 0.0005	0.512 ± 0.0005	0.513 ± 0.0002	0.545 ± 0.0008	0.549 ± 0.0008	0.555 ± 0.0009
FWHM$_{peak}$ (nm^{-1})	0.153 ± 0.0015	0.151 ± 0.0014	0.101 ± 0.0009	0.097 ± 0.0004	0.150 ± 0.0019	0.146 ± 0.0019	0.144 ± 0.0019
Correction exponent (n)	1.3	1.3	0.6	0.85	0.8	0.8	0.8
Degree of anisotropy	0.950 ± 0.003	0.950 ± 0.004	0.950 ± 0.004	0.980 ± 0.002	0.850 ± 0.006	0.870 ± 0.006	0.860 ± 0.004

ACKNOWLEDGMENTS

This research activity was funded by the Swiss Nanoscience Institute (SNI) through the applied research project DICANS, a collaborative initiative between the Biomaterials Science Center (BMC) of the University of Basel, the Paul Scherrer Institut (PSI), the University of Applied Sciences and Arts Northwestern Switzerland (FHNW), and Concentris GmbH. The authors thank O. Häfeli (FHNW Windisch) for the injection molding, K. Jefimovs (EMPA Dübendorf) and A. Stumpp (FHNW Windisch) for laser micro-machining of the mold, as well as X. Donath (PSI, Villigen) for support at the beamline. Experiments were performed on the cSAXS beamline at the Swiss Light Source, Paul Scherrer Institut, Villigen, Switzerland.

[1]L. Sawyer, D. Grubb, and G. Meyers, *Polymer Microscopy* (Springer Science, New York, 2008), Vol. 2.
[2]J.-W. Housmans, M. Gahleitner, W. M. P. Gerrit, and H. Meijer, Polymer **50**, 2304 (2009).
[3]W. Michaeli and M. Bussmann, *Shear-Induced Morphology Prediction in Injection Moulded Semi Crystalline Thermoplastics* (2005).
[4]H. Mavridis, A. Hrymak, and J. Vlachopoulos, Polym. Eng. Sci. **26**, 449 (1986).
[5]M. Gahleitner, J. Wolfschwenger, C. Bachner, K. Bernreitner, and W. Neißl, J. Appl. Polym. Sci. **61**, 649 (1996).
[6]M. Gahleitner, C. Bachner, E. Ratajski, G. Rohaczek, and W. Neißl, J. Appl. Polym. Sci. **73**, 2507 (1999).
[7]Z. Tadmor, J. Appl. Polym. Sci. **18**, 1753 (1974).
[8]M. Kantz, H. Newman, and F. Stigale, J. Appl. Polym. Sci. **16**, 1249 (1972).
[9]H. Ito, Y. Yagisawa, T. Saito, T. Yashuhara, T. Kikutani, and Y. Yamagiwa, Theor. Appl. Mech. Jpn. **54**, 263 (2005).
[10]O. Bunk, M. Bech, T. Jensen, R. Feidenhans'l, T. Binderup, A. Menzel, and F. Pfeiffer, New J. Phys. **11**, 123016 (2009).
[11]Y. D. Wang and M. Cakmak, Polymer **42**, 3731 (2001).
[12]Y. D. Wang and M. Cakmak, Polymer **42**, 4233 (2001).
[13]P. Urwyler, O. Häfeli, H. Schift, J. Gobrecht, F. Battiston, and B. Müller, Procedia Eng. **5**, 347 (2010).
[14]M. C. Garcia-Gutierrez, A. Nogales, J. J. Hernandez, D. R. Rueda, and T. A. Ezquerra, Opt. Pura Apl. **40**, 195 (2007).
[15]P.-W. Zhu and G. Edward, Macromol. Mater. Eng. **288**, 304 (2003).

Biointerphases (2012) 7:6
DOI 10.1007/s13758-011-0006-6

IN FOCUS: NANOMEDICINE - ARTICLE

Nano-Mechanical Transduction of Polymer Micro-Cantilevers to Detect Bio-Molecular Interactions

Prabitha Urwyler · Joachim Köser · Helmut Schift · Jens Gobrecht · Bert Müller

Received: 6 October 2011 / Accepted: 18 November 2011

Abstract Using variothermal polymer micro-injection molding, disposable arrays of eight polymer micro-cantilevers each 500 μm long, 100 μm wide and 25 μm thick were fabricated. The present study took advantage of an easy flow grade polypropylene. After gold coating for optical read-out and asymmetrical sensitization, the arrays were introduced into the Cantisens® Research system to perform mechanical and functional testing. We demonstrate that polypropylene cantilevers can be used as biosensors for medical purposes in the same manner as the established silicon ones to detect single-stranded DNA sequences and metal ions in real-time. A differential signal of 7 nm was detected for the hybridization of 1 μM complementary DNA sequences. For 100 nM copper ions the differential signal was found to be (36 ± 5) nm. Nano-mechanical sensing of medically relevant, nanometer-size species is essential for fast and efficient diagnosis.

Abbreviations

MEMS	Micro-electro-mechanical systems
NEMS	Nano-electro-mechanical systems
μC	Micro-cantilever
PP	Polypropylene
μIM	Micro-injection molding
ssDNA	Single-stranded DNA
GSH	Glutathione
MCH	Mercaptohexanol
SAM	Self-assembled monolayer

1 Introduction

Medical diagnostics is a vital part of routine clinical practice. Monitoring human biological systems at the molecular level using nanodevices and nanostructures brings nanotechnology closer to nanomedicine. For better diagnosis, nanometer-size species, i.e. biomolecules, have to be recognized with high reliability, high sensitivity and selectivity within short periods of time. Size reduction of diagnostic devices decreases the amount of analyte, thereby leading to faster analysis. Therefore, micro and nano electro-mechanical systems (MEMS and NEMS) have attracted much interest for biomedical applications, often termed as nanoanalytics in the field of nanomedicine.

Micro-fabricated cantilevers and cantilever arrays belong to the promising biosensors under MEMS. For example, their high sensitivity and selectivity was demonstrated analyzing DNA sequences [1–3]. They can also operate as artificial olfactory and gustatory organs with sound performance [4–6]. The static working principle of

This article is part of the Topical Collection "In Focus: Nanomedicine".

P. Urwyler · B. Müller (✉)
Biomaterials Science Center, University of Basel,
c/o University Hospital, 4031 Basel, Switzerland
e-mail: bert.mueller@unibas.ch

P. Urwyler · H. Schift · J. Gobrecht
Laboratory for Micro- and Nanotechnology,
Paul Scherrer Institut, 5232 Villigen PSI, Switzerland

J. Köser
Institute of Chemistry and Bioanalytics,
University of Applied Sciences Northwestern Switzerland,
4132 Muttenz, Switzerland

J. Gobrecht
Institute of Polymer Nanotechnology,
University of Applied Sciences Northwestern Switzerland,
5210 Windisch, Switzerland

Published online: 09 February 2012

such nanomechanical transducers comprises the conversion of the (bio) chemical reaction of interest on the active side of the cantilever into surface stress thus leading to the bending of the cantilever [7]. The optical readout ensures the detection of this bending with nanometer precision. In order to achieve selectivity, well-selected recognition elements are integrated on the active side of the micro-cantilever (μC). In general, silicon technology has been applied to prepare these μC arrays, which are commonly designed for single usage. Multiple uses for clinical applications are in most cases impossible. Therefore, such sensor systems are relatively expensive. Replacing the silicon-based μC arrays by means of low-cost injection-molded arrays from appropriate polymers is crucial not only to lower the costs but also to open up a broad spectrum of applications, for example in intensive care units [6, 8].

The substitution of silicon by a polymer such as polypropylene (PP), seems to be reasonable since the sensitivity of the cantilever sensor (deflection Δ_z, differential surface stress $\Delta\sigma_{\text{surface}}$) depends on the mechanical parameters (Young's modulus E and Poisson's ratio v) and the geometry (length L, thickness t) as demonstrated more than a century ago [9].

$$\Delta_z = \frac{3(1-v)L^2}{Et^2}(\Delta\sigma_{\text{surface}})$$

Simple estimations show that typical polymer cantilevers can retain the sensitivity of silicon cantilevers despite a factor of 5–10 increase in their thickness. Therefore, micro-injection molding (μIM) can be applied to fabricate low-cost disposable μC arrays [10]. μIM allows an easy switch to comparable alternative polymers and for surface micro-structuring by means of methods such as embossing. Compared to the distinct single crystalline Si cantilevers, the polymer μCs within an array exhibit slight variation in geometry. For that reason, the polymer μC arrays have to be tested for their suitability in biomedicine. This includes the direct comparison with the well established Si-cantilever experiments [11–13].

Rather simple examples are the hybridization of DNA fragments with single-stranded DNA (ssDNA) or oligonucleotide that are covalently immobilized on a gold-coated cantilever taking advantage of thiol chemistry [1, 2, 11–14].

The metal ion sensing applications of the polymer μCs was studied using glutathione (GSH) monolayer's affinity for copper ions. Copper plays an essential role in human physiology. Copper ions are considered as multifunctional participating in a broad spectrum of intracellular processes under normal and pathologic conditions. The intracellular concentration of copper is tightly controlled. Exchangeable copper in cytosol is bound to small protein carriers called metallochaperones like GSH. GSH, a tripeptide from glycine, cysteine and glutamate, is the most abundant non-protein thiol-bearing molecule of mammalian cells and is involved in many physiological processes [15–17]. GSH is known to interact with ions and heavy metals, and is capable to organize on gold surfaces as self assembled monolayers (SAMs) [18]. SAMs serve as sensitive sensing layer for cantilever based sensors. Gold coating can be performed for silicon and polymer in similar manner. In both cases, experience exists as gold has been deposited as reflection layer for optical read-out of cantilever deflection. Nevertheless, it has to be demonstrated that polymer cantilever sensors reach the desired selectivity, sensitivity, and reliability for the detection of relevant bio-molecules and metal ions.

2 Materials and Methods

2.1 Cantilever Fabrication

Arrays of eight polymeric μCs (see Fig. 1) were fabricated using variothermal μIM. The setup was similar as described in [10], consisting of a metal (Polmax Uddeholm) mold insert (90 × 100 mm^2) mounted in the clamping unit with millimeter-size cavities, which was closed by a flat counterpart (mirror unit) containing the injection gate. The molding tool was installed in an Arburg 320 Allrounder (Arburg, Lossburg, Germany) with a maximum clamping force of 600 kN. The mirror unit of the molding tool, a polished steel surface ensured an optically flat and smooth surface. On the tool side 16 branches of 2.5 mm wide and 60 mm long channels with semi-cylindrical shape were ordered around the central point opposite to the injection gate, all ending in 3.5 × 2.5 × 0.5 mm^3 cavities representing the μC array holder cavities (Fig. 1d).

The eight nominally 25 μm-deep, 500 μm-long and 100 μm-wide μC mold cavities were laser ablated between the holder cavity and millimeter-long, 20 × 20 μm^2-wide venting channels. Due to the laser ablation process, the μC mold cavities are not rectangular. The cross-section exhibits a trapezoid form (Fig. 1b), with a widening of about 10 μm on each side from the laser-ablated bottom of the cavity to the top, which during injection molding is formed by the mirror side of the molding tool. Due to fabrication tolerances, the widths of the individual μC mold cavities vary from 83 to 88 μm, leading to variations in the mechanical behavior. For variothermal heating, heat cartridges were placed directly below and above the μC mold cavities, i.e. on both the tool and the mirror sides, thus enabling localized heating above the tool temperature. As polymer, an easy flow grade polypropylene (PP Metocene HM 648T, LyondellBasell, Bayreuth, Germany) served for the studies presented in this paper. The ejector pins in each channel ensured easy demolding. The parts were manually

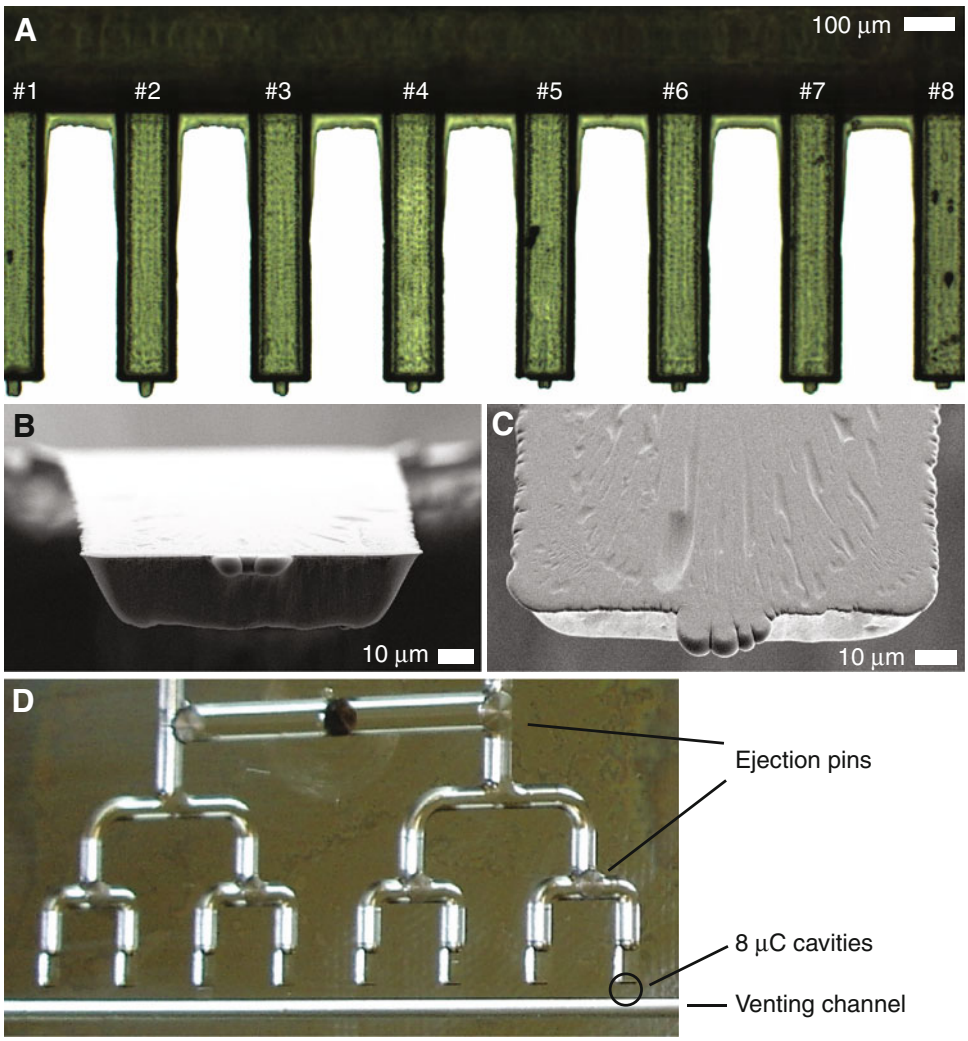

Fig. 1 Optical micrograph of a variothermal micro-injection molded PP µC array, each cantilever is 500 µm long, 100 µm wide and 25 µm thin (**a**), SEM micrograph of the trapezoidal form of the PP µC (**b**), SEM micrograph of the surface of the PP µC (**c**), photograph showing a part of the mold insert (**d**)

removed from the mold, i.e. no mold release agent was applied. The process parameters were similar to the one's given in Ref. [10], i.e. melt temperature 200°C, tool temperature 40°C and injection speed 9 cm^3/s. Using variothermal µIM process parameters (increase of 30 K over tool temperature at the beginning of each molding cycle), the complete filling of the high-aspect-ratio microcavities was achieved, as demonstrated by the microscopy images in Fig. 1. The µC arrays were produced in batches of 20 arrays. Further details on the fabrication of PP and other polymeric µCs will be given in a forthcoming publication in an engineering journal.

2.2 Cantilever Functionalization

To functionalize cantilevers with receptor molecules and also to ensure sufficient reflectivity of the laser signal, the PP µCs were coated on the replicated mirror side with a 4 nm-thin chromium film (Umicore; Code 0702723, Cr 99.99%, Flakes 2.8–4.7 mm) followed by a 20 nm-thin gold film (Umicore; Code P0481088, Au 99.99%, 2 mm wire) using a thermal evaporator (Balzers BAE 250, Balzers, Liechtenstein). The film thickness was controlled by means of the quartz crystal microbalance integrated in the evaporation system.

Prior to functionalization, the µCs were treated in a UV/Ozone cleaner (UV Clean Model 13550, Boekel Scientific, Feasterville, PA). This procedure yields a well-defined gold surface, which is crucial for the thiol immobilization. To avoid chemical degradation of the PP, the UV-ozone treatment was limited to a period of 20 min.

The µCs were functionalized by immersing them for a time period of 30 min in glass capillaries filled with experiment specific functionalization solution using the Cantisens® FU-401 unit (Concentris GmbH, Basel, Switzerland). In order to prevent any evaporation of the experiment specific functionalization solution, the procedure was carried out in humidified atmosphere.

For the copper ion sensing experiments, µCs #2, #4, #6, #8 were coated with glutathione (GSH, Sigma Aldrich, Buchs, Switzerland) in Cu-functionalization buffer solution

(100 mM NaCl, 10 mM Tris) [11], while the other four bare μCs served as references.

For the DNA hybridization experiments, μCs #1, #2, #5, #6 were functionalized with ssDNA thiol-Nl4-3 sequence (Microsynth AG, Balgach, Switzerland), and μCs #3, #4, #7, #8 with ssDNA thiol-Sf162 (Microsynth AG, Balgach, Switzerland) in DNA-functionalization buffer solution (200 nM NaCl, 20 mM Tris), as described in detail earlier [11]. In short, μCs #1, #2, #5 and #6 were functionalized first, followed by μCs #3, #4, #7, and #8 according to the geometry of the functionalization unit generally applied for Si cantilevers. The human immunodeficiency virus type 1 (HIV-1) strain thiol-Sf162 (CAT ACA ACA GGA AGA ATA ATA GGA G) and thiol-Nl4-3 (GTT ACA ATA GGA AAA ATA GGA A) were used as the sensing sequences.

2.3 Mechanical Characterization of Cantilevers

The gold-coated PP μCs were introduced into the water-filled measurement cell maintained at a temperature of 25°C. Using the optional liquid handling system from the integrated temperature control in the Cantisens® system, a temperature profile program under static conditions was setup. The temperature was increased with a rate of 0.2 K/s from 25 to 30°C, then holding constant for 240 s and then decreased back to 25°C with a rate of −0.2 K/s. Subsequently, such a cycle was performed using a temperature difference of 10 K, i.e. from 25 to 35°C and back to 25°C (see Fig. 2).

2.4 Monitoring Surface Stress During Thiol Adsorption

The characterization of thiol functionalization on gold-coated PP μCs was conducted applying a constant flow of 0.42 μL/s at a temperature of 25°C. 100 μL of 0.1 mM mercaptohexanol (MCH, Sigma Aldrich, Buchs, Switzerland) diluted in water was injected into the pumping loop and the cantilever bending during the real-time chemisorption of thiol on the gold was recorded. This is a test for the mechanical behaviour of the cantilevers when a chemical reaction takes place at the surface.

2.5 Analytical Procedure

The measurements were done using the Cantisens® Research platform, which allows for real-time experiments. The experiments (copper sensing and DNA hybridization) were conducted with a constant flow (0.42 μL/s) at a temperature of 30°C. For MCH treatment, 0.1 mM of MCH diluted in the experiment specific running buffer solution, i.e. Cu-running buffer and DNA-running buffer, was prepared and introduced into the measurement cell. The measurement cell and the connecting tubes of the pumping loop including valves were cleaned before each injection.

The glutathione-functionalized μCs were rinsed for several minutes in the Cu-running buffer (100 mM NaCl, 0.5 mM EDTA, 10 mM Tris, 0.005% Tween 20, pH 7.5) to remove excess adsorbed glutathione. The sample (analyte) solution was prepared dissolving copper chloride ($CuCl_2$, Sigma Aldrich, Buchs, Switzerland) in the Tris buffer (100 mM NaCl, 10 mM Tris, 0.005% Tween 20, pH 7.5) to a final concentration of 100 nM.

The sample (analyte) solution used in the DNA hybridization experiment was 1 μM complementary Sf162 diluted in the DNA-running buffer (1 M NaCl, 20 mM Tris pH 7.2, 0.005% Tween). The μCs were regenerated after each experiment washing them with 30% urea (Sigma Aldrich, Buchs, Switzerland) solution, which completely removes hybridized complementary ssDNA [1].

3 Results

3.1 Mechanical Characterization

For applying cantilevers in sensing applications, it is important that the cantilevers bend homogenously, thereby requiring their characterization. The mechanical behavior of the μCs was tested by thermally induced bending of the asymmetric cantilever, often termed heat test. The heat tests included a temperature cycle from 25 to 30°C and 25 to 35°C as described above. Due to the difference in the thermal expansion of the 24-nm thin metal layer and the 25-μm thick PP layer, compressive stress is generated resulting in a deflection. The deflection from the central four μCs (#3, #4, #5, #6) is almost twice that of the outer four μCs (#1, #2, #7, #8). For a temperature difference of 5 and 10 K, the maximum deflection for the central PP μCs in water corresponds to (365 ± 20) nm and (800 ± 50) nm, respectively (cp. Fig. 2).

3.2 Thiol Adsorption

Creation of homogeneous monolayers on cantilever surfaces forms the basis of most sensing experiments. The thiol compounds have a high affinity for the gold-coated surface of the μCs and bind to the gold forming a densely packed SAM. The deflection caused by injection of 0.1 mM MCH is shown in Fig. 3. μC #8 was omitted due to its insufficient reflectivity for read-out. Surface stress generated during the growth of the self-assembled thiol monolayer led to significant cantilever bending. A maximum deflection of (110 ± 10) nm was recorded in real-time for the μCs (with exception of μC #5). Using the Stoney formula [9, 19], the differential surface stress was

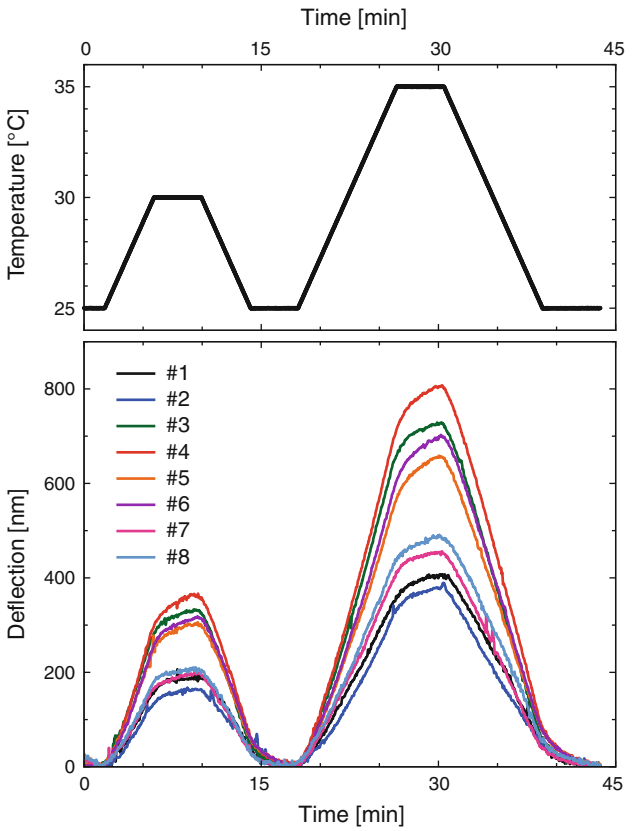

Fig. 2 The graph on the *top* shows the temperature cycle and the graph *below* shows the response of the variothermal molded PP μCs

calculated to a value of (0.28 ± 0.03) N/m^{-1}. The PP μCs bend continuously until saturation lasting for a minute. The SAM formation monitored in real-time is a fast process as seen in Fig. 3 which can be interesting for biomedical applications.

3.3 Copper Sensing

When copper ions are injected in the measurement chamber, the glutathione-functionalized cantilevers bind the divalent copper ion and generate a related deflection signal. The injection of 100 μL of 100 nM $CuCl_2$ causes a shift in the differential signal of (36 ± 5) nm corresponding to a differential surface stress of (0.090 ± 0.002) N/m^{-1} as clearly shown by the data in Fig. 4. The decrease in deflection after 5 min is due to the instability of the experimental setup and lies within the error bars. Figure 4a shows the deflection of the individual μCs including the reference μCs (#2, #4, #6, #8) and signal μCs (#1, #3, #5, #7).

3.4 Detection of DNA Hybridization

DNA hybridization is caused by the complementary interaction between probe DNA and sample DNA [14]. The difference between the average signal μCs (#3, #4, #7,

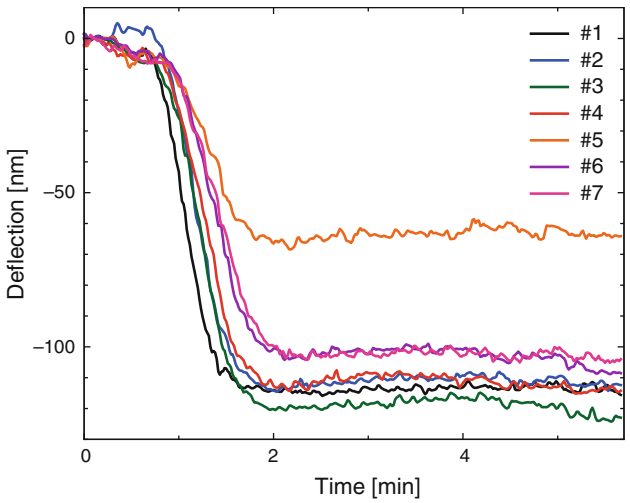

Fig. 3 Surface stress generated during the formation of MCH SAM on the gold layer on the active side of the PP μCs

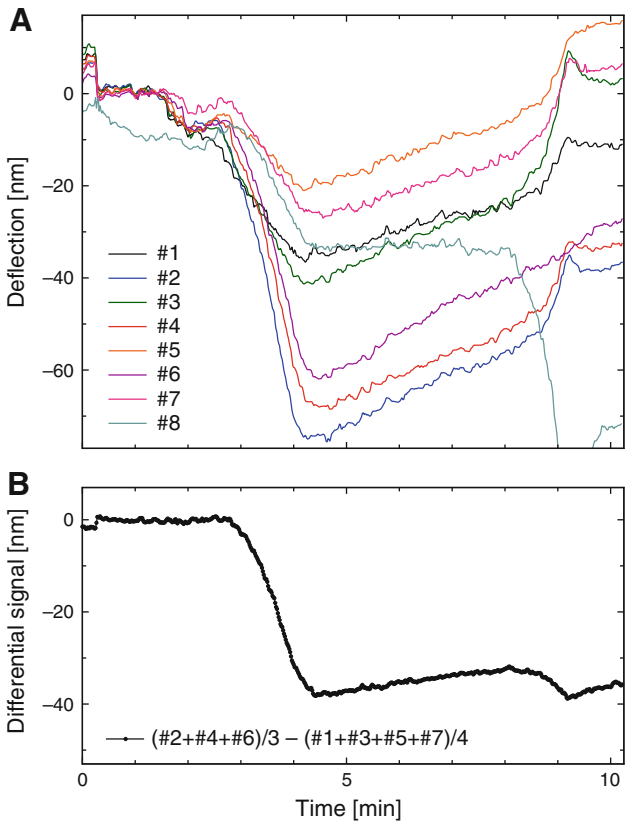

Fig. 4 Deflection of the reference μCs and GSH-functionalized PP μCs upon $CuCl_2$ injection (**a**), Differential signal from Cu^{2+} ions binding to GSH-functionalized PP μCs (**b**)

#8) deflection and the average reference μCs (#1, #2, #5, #6) deflection is shown in Fig. 5. The differential signal is generally required because of thermal drifts and unspecific interactions. The first injection of 100 μL of 1 μM complementary Sf162 sequence gives a signal of 7 nm

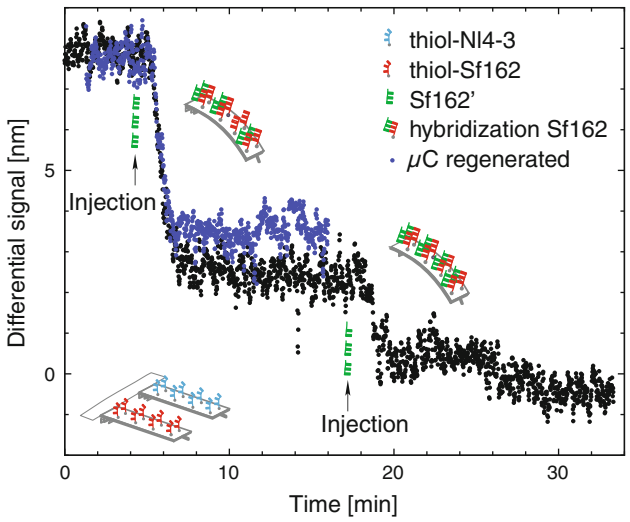

Fig. 5 Differential deflection upon hybridization of the complementary ssDNA sequence with the thiol-ssDNA sequence attached on the gold

($\Delta\sigma_{surface} = 0.02$ N/m^{-1}), which is comparable to the signals achieved with Si cantilevers. The differential deflection of 7 nm corresponds to 25% of differential deflection obtained with the 1 μm-thin silicon cantilevers [11, 14]. A second injection of the same complementary sequence was a control for measuring the saturation level of the first injection and led to an additional 1.5 nm differential signal. After regeneration, the DNA experiments give the same signal within the error bars. Figure 5 also shows the differential deflection signal of DNA hybridisation after regeneration. The result demonstrates the application of cantilever sensors for the detection of ssDNA sequences via their hybridisation with sensing ssDNA immobilised on the cantilever. It is important that the reference cantilevers are as similar to the sensing cantilever as possible. Note that a bare cantilever cannot be used, as the sample DNA interacts with the bare cantilever leading to a bending signal. Therefore, similar DNA sequences have to be used as reference. The HIV-1 sequences Nl4-3 and Sf162 are 70–80% homologous to each other. Hence Nl4-3 sequence was used as the reference. Using homologous sequences, the specificity of the DNA hybridization can be detected and distinguished by the cantilever sensors.

4 Discussion

Complete filling of the 25 μm thick, 500 μm long cavities using variothermal μIM was possible using the easy flow grade PP. The 25 μm-thick PP μCs are far too thick compared to the estimated 5–10 μm thickness needed for direct comparison to the standard 1 μm-thick Si μC. According to the Stoney formula, their mechanical behavior would correspond to 4 μm thin Si μCs. However, our results show that sufficient selectivity can be achieved with the 25 μm-thick PP μC, too. With the current setup and parameters, μCs much thinner than 25 μm are difficult to achieve, particularly if tight homogeneity aspects have to be met. However, better results can be expected with optimized temperature gradients within the mold and possible thermal treatment procedures after appropriate demolding. The molding process can be further tuned to incorporate other biocompatible polymers, however, only if similar flow properties can be met. The current aim is rather to improve sensitivity by implementing surface structures than by further reducing the cantilever thickness. This concept was demonstrated in Ref. [10], but will be investigated in more detail in future research. Further advances in polymer μCs can be promising in developing sensors with suitable sensitivity and selectivity.

In the heat tests, upon temperature change, the biphasic μC deflects due to the bending moment generated by the different thermal expansions of the two materials [11, 20]. We have shown that PP μCs with a thin gold film on one side undergo measurable bending in response to temperature changes. The deflection signal with the variothermal injection molded μCs is larger as compared to the ones molded in a non-variothermal mode [10]. These gold-coated μCs have the potential to distinguish effects of temperature and can be used in applications requiring high precision thermal sensitivity. The difference in deflection of the outer cantilevers to the central ones is a severe drawback. It might be significantly reduced identifying suitable temperature gradients within the mold and applying appropriate demolding procedures. Furthermore, the fixation mechanism of the cantilever array might lead to a tilt that stiffens the outer cantilevers. Therefore the fixation should be optimized. It must be noted that the deflections shown in the heat tests are huge as compared to the deflections observed in biosensing experiments. Mechanical characterization of each disposable PP μC array is necessary before meaningful experiments can be carried out.

The formation of SAMs is of great interest in the field of surface science. SAMs of highly ordered and oriented alkane thiolates provide a prominent, flexible, and convenient way to generate well-defined organic surfaces with useful and highly alterable chemical functionalities displayed at the exposed interface [21]. It has been shown that the deflection during the chemisorption of thiols is due to the surface stress and the thermal effects involved in the exothermic thiol SAM formation are negligible [19]. A clean and smooth gold surface is a pre-requisite for uniform thiol adsorption. The large deviation in the deflection of μC #5, for example resulted from

inappropriate gold coating (see Fig. 1a). The degradation of the PP μC surface and the gold coating during the UV/ozone treatment cannot be ruled out either. The thiol adsorption measurements elucidate the necessity of calibration before reproducible experiments can be performed, reliably. The sensing applications of μCs including artificial noses needs calibration even for silicon.

The ion sensing properties of the GSH SAMs are demonstrated with the copper sensing experiments. Sensing properties of GSH SAMs are promising and can be extended to further applications such as metal concentration after chemotherapies.

Increased levels of copper in cerebrospinal fluid in patients with Alzheimer's disease have been found [22]. Further experimental studies would aid the discovery of effective Cu biomarkers and the generation of new options for early intervention in copper-related health disorders.

Fritz et al. [1] already showed that the hybridization of complementary DNA is measurable giving rise to a surface stress change of 1 mN/m and a mismatch between two 12-mer oligonucleotides is clearly detectable. The detection of ssDNA hybridization was chosen as a model experiment to demonstrate the effectiveness of PP μCs as biosensors. MCH served as a blocking molecule between the immobilized thiolated ssDNA molecules to prevent unspecific interaction of complementary DNA with the gold surface. Two 18-mer oligonucleotides, which are 70–80% homologous, were used in our hybridization experiments as compared to the 12-mer oligonucleotides reported earlier [1, 2]. For optimal distinction of hybridization between the 70 and 80% homologous strands, the temperature of the experiments were elevated to 30°C. The higher temperature helps to gain specificity of DNA hybridization with longer nucleotides. The response of PP μCs during the hybridization of complementary ssDNA with the probe ssDNA is shown. The bending direction of the μCs (bend up or down) during hybridization is consistent with the Si μCs. However, the magnitude of the displacement is four times smaller than for the Si μCs which corresponds to their higher stiffness coming from a significantly larger thickness of the polymer μCs. The sensitivity of the cantilever sensing is determined by the number of the binding events that give rise to the surface stress. With 18-mer oligonucleotides, the number of DNA molecules per cantilever is smaller than 10^{10} probes per cantilever as mentioned earlier [2]. The reduced number of DNA molecules per cantilever can lead to a reduction in signal but increase in sensitivity. The cantilever surface with ssDNA probes can open options for detection of target genes or antigens. It can be further extended to measure single nucleotide polymorphisms with μC sensors in a fast and easy way.

5 Conclusions

Within many areas of medicine, there has been a constant need for technical developments and sophisticated methods. The development of a simple, portable, clinical diagnostic device that can perform a comprehensive range of tests, inexpensively, and give results within a few minutes has been a dream of biosensing research groups for many years. Such a device will have the capability to make diagnoses, monitor critical clinical indicators and tailor treatments, accordingly. Since results are available on site, remedial action can be initiated. With the polymer microcantilevers shown here, a first step towards this goal is demonstrated. In comparison to the silicon cantilevers used until now, comparable results can be achieved. The advantage of our technique is that a range of polymers can be used for injection molding thereby adapting the mechanical properties of the cantilever sensor to the desired application. As an added advantage, the polymer μCs can easily be surface patterned [10] to increase sensitivity or to enhance specific interaction with cells.

Cantilevers sense surface-associated processes like conformational changes or molecular interactions. The rapid, real-time detection of interactions/biomolecules is clearly an advantage of the label-free biosensor, allowing further applications in basic research and sensing [11, 23, 24]. μC biosensors hold promising perspective in the applications of medical diagnosis through the development of miniaturized, low-cost sensor platforms. The μIM process provides a fast, inexpensive and reliable method to obtain arrays of μCs [10]. With eight cantilevers in an array, eight different species or bio-molecular interactions can be detected with no extra label or tag. PP μC arrays have proven their selectivity to detect DNA sequences and distinguish homologous sequences. Currently, the detection limit lies in micro-molar concentrations, but can be significantly lowered to nano-molar concentrations reducing cantilever thickness. In future cantilever sensors with improved design, tooling and process parameters, can lead to medical diagnostic devices that are portable and inexpensive, useful in the detection and diagnosis of human diseases.

This activity is funded by the Swiss Nanoscience Institute through the applied research project DICANS a collaborative initiative between the Biomaterials Science Center (BMC), Paul Scherrer Institute (PSI), University of Applied Sciences Northwestern Switzerland (FHNW) and Concentris GmbH. We thank the members from the Laboratory for Micro- and Nanotechnology (LMN-PSI), Institute for Polymer Nanotechnology (INKA), FHNW (especially Oskar Häfeli for injection molding), and EMPA Dübendorf (Konstantins Jefimovs for laser micro-ablation of metal molds) for their technical assistance. The

cantilever measurements were performed at the Institute for Chemistry and Bioanalytics lab at FHNW Muttenz with the Cantisens® Research platform.

References

1. Fritz J (2000) Science 288:316
2. Mckendry R, Zhang J, Arntz Y, Strunz T, Hegner M, Lang H, Baller M, Certa U, Meyer E, Güntherodt H-J, Gerber C (2002) PNAS 99(15):9783–9788
3. Zhang J, Lang H, Huber F, Bietschi A, Grange W, Certa U, Mckendry R, Güntherodt H-J, Hegner M, Gerber C (2006) Nat Nanotechnol 1:214–220
4. Baller M, Lang H, Fritz J, Gerber C, Gimzewski J, Drechsler U, Rothuizen H, Despont H, Vettiger P, Battiston F, Ramseyer J, Fornaro P, Meyer E, Güntherodt H-J (2000) Ultramicroscopy 82:1–9
5. Battison F, Ramseyer J, Lang H, Baller M, Gerber C, Gimzewski J, Meyer E, Güntherodt H-J (2001) Sens Actuators B 77:122–131
6. Schmid D, Lang H, Marsch S, Gerber C, Hunziker P (2008) Eur J Nanomed 1:44–47
7. Alvarez M, Lechuga L (2010) Analyst 135:827–836
8. Ting C, Nanji A (1998) Can Med Assoc J 138:23–26
9. Stoney G (1909) Proc Royal Soc London Ser A 82(553):172–175
10. Urwyler P, Schift H, Gobrecht J, Häfeli O, Altana M, Battiston F, Müller B (2011) Sens Actuators A: Phys 172(1):2–8
11. Köser J, Shahgaldian P, Bammerlin M, Battiston F, Pieles U (2007) J Phys 61:612–617
12. Hansen K, Thundat T (2005) Methods 37:57–64
13. Ziegler C (2004) Anal Bioanal Chem 379:946–959
14. Kim D, Kang D (2008) Sensors 8:6605–6641
15. Ubiyvovk V, Ananin V, Malyshev A, Kang H, Sibirny A (2011) BMC Biotechnol 11(8):12
16. Davidson T, Ke Q, Costa M (2007) Selected molecular mechanisms of metal toxicity and carcinogenicity. Elsevier, Burlington
17. Smith C, Jones D, Guenthner T, Lash L, Lauterburg B (1996) Toxicol Appl Pharmacol 140:1–12
18. Bieri M, Bürgi T (2006) Phys Chem Chem Phys 8(4):20
19. Berger R, Delamarche E, Lang P, Gerber C, Gimzewski J, Meyer E, Güntherodt H-J (1997) Science 276:2021–2024
20. Chu W-H, Mehregany M, Mullen R (1993) J Micromech Microeng 3:4–7
21. Yuan M, Zhan S, Zhou X, Liu Y, Feng L, Lin Y, Zhang Z, Hu J (2008) Langmuir 24:8707–8710
22. Iakovidis I, Delimaris I, Piperakis S (2011) Mol Biol Int. doi: 10.4061/2011/594529
23. Velanki S, Ji H-F (2006) Meas Sci Technol 17:2964–2968
24. Ghatkeser M, Lang H, Gerber C, Hegner M, Braun T (2008) PLoS ONE 3(11):e3610

CONCLUSIONS AND OUTLOOK

Cantilevers deform through surface-associated processes including conformational changes of adherent species and adsorption of molecules. The rapid, real-time detection of interactions/molecules is clearly a main advantage of this label-free biosensor allowing applications in basic research and beyond. μC biosensors hold promising perspectives in medical diagnosis through the development of miniaturized, low-cost sensor platforms.

First, iso- and vario-thermal μIM processes provide a fast, inexpensive, and reliable method to obtain polymeric μC arrays with reasonable properties for biomedical applications. With eight cantilevers in an array, up to eight different species can be simultaneously detected with no extra label or tag. The UVO treatments used for surface-cleanliness of μCs can significantly influence their physical and chemical properties. The exposure times of up to 20 minutes can be used for UVO-based cleaning since the mechanical properties of the μC do not significantly change. Nanometer-thin gold coatings, often deposited to obtain reasonable laser beam reflectivity, do not prevent the μC degradation, but retard the UVO-induced modification. The thiol-gold binding tests demonstrate that the polymer micro-cantilevers are highly sensitive surface stress monitors. Mechanical and functional tests imply that these polymer μCs are mechanically compliant for use in biochemistry and biomedicine.

Second, the spatially resolved SAXS and WAXS data elucidate that the μCs are homogeneous in the scanning directions perpendicular to the beam. Their crystalline structure, however, exhibits a strong anisotropy. Both crystallinity and anisotropy can be controlled by changing the mold temperature.

Third, vario-thermal injection-molded PP μC arrays have proven their selectivity to detect DNA sequences and distinguish homologous sequences. Currently, the detection limit lies in micro-molar concentrations, but can be significantly lowered to nano-molar concentrations reducing cantilever thickness.

Fourth, the advantage of our approach is that a range of polymers can be used for injection molding thereby adapting the mechanical properties of the cantilever sensor to the desired application. As an added advantage, the polymer μCs can easily be surface patterned on the micro- and nanometer scales to increase sensitivity or to enhance specific interaction with biological cells. It is expected that by choosing appropriate sizes and orientations of the surface microstructures, the mechanical properties of individual μCs with identical outlines can be significantly modified. Surface structuring can also tailor cell locomotion, adhesion and spreading, which are closely related to the contractile cell forces to be quantified. The μCs patterning can be established for a range of cantilever designs. In addition, by

modifying the μC surface morphology or chemistry one can mimic implant surfaces and can compare the influence on the cell response. Thus, the microstructured μC array sensors will support the selection of advanced surface-modified substrates and medical implant surfaces.

Future perspectives

Thinner cantilevers would be a valuable contribution for sensing. Variotherm molds and methods achieved within the scope of this thesis can be fine tuned to achieve thinner cantilevers. While fabricating thinner cantilevers, the curling and the warpage has to be taken care off. One of shortcoming on the manufacturing side was the amount of flash on the μC part and this could possibly be reduced or eliminated by increasing the clamping pressure of the molding machine. Automation of the demolding process, packaging and finishing should be considered as a step for commercialisation of the injection molded cantilevers.

Cantilevers with varying thickness within an array are desired for bio-molecular applications. This is difficult to be achieved with Si-based arrays due to limitations of the fabrication process. Injection molding would be the right way to realize μCs of different thickness.

The mechanical changes induced by surface structuring of the μCs with respect to biosensing can be explored further. Different topographical structures can change the stiffness of the cantilever and thereby its sensitivity. A comparison of sensing experiments on plain and micro- and nanostructured μCs will open new avenues. Modifying the surface morphology one can mimic implant surfaces. The binding or adhesion of proteins and cell-materials interactions can be studied using the structured μCs. This approach promises the potential for quantitative determination of mechanical force in living cells and is expected to bridge the gap between cellular behavior and materials.

In future cantilever sensors with improved design, tooling and process parameters, can lead to medical diagnostic devices that are portable and inexpensive, useful in the detection and diagnosis of human diseases or in environmental monitoring. Once successfully established, the polymer-based μC systems will permit to gain major cost reductions and to address further applications in the field of biomedicine.

Mittelstrasse 2
3073 Gümligen
Switzerland

Tel: +41 31 954 09 59
Mobile: +41 79 927 96 03
E-Mail: prabitha@gmx.ch

Prabitha Urwyler

Personal

Date of Birth	03.03.1974
Place of Birth	Mangalore, India
Civil Status	Married, 2 children (Date of Birth: 29.10.2002, 09.06.2005)
Nationality	Swiss, Indian (Overseas Citizenship of India)
Place of Origin	Aarwangen, Canton Bern, Switzerland
Languages	English, German, Hindi, Kannada, Tulu

Education and Academic Career

2008 – 2012	Doctoral Studies, Biomaterials Science Center, University of Basel, Switzerland PhD Thesis: "Polymeric micro-cantilever sensors for biomedical applications"
2008	Degree of Master of Science (M.Sc. – Biomedical Engineering) University of Bern, Bern, Switzerland
2006 – 2008	Engineering Postgraduate Studies, Medical Faculty, University Bern, Switzerland Master Thesis: "Biomechanical Characterisation of Annulus and Nucleus repair methods"
1995	Degree of Bachelor of Technology (B.Tech – Computer Science and Engineering), Mangalore University, Mangalore, India
1991 – 1995	Engineering Studies, Department of Computer Science, NMAMIT, Nitte, Mangalore University, India

Research & Work Experience

2012- present	University of Basel, Biomaterials Science Center, Basel, Switzerland Post-Doctoral Associate
2008 - 2012	Paul Scherrer Institut, Laboratory for Micro- and Nanotechnology, Villigen PSI, Switzerland PhD Candidate / Research Associate
2007 - 2008	University of Bern, Institute for Surgical Technology and Biomechanics, Bern, Switzerland, M.Sc Candidate
2010 - present	sda Informatik, Zurich, Switzerland Software Consultant / Free-lancer
1997 - 2008	Schweizerische Depeschenagentur (SDA – ATS), Bern, Switzerland Software Engineer
1997	SoftData, Bremgarten bei Bern, Switzerland Software Engineer
1995 - 1997	Melstar Information Technologies Ltd, Mumbai, India Software Developer

Supervisory Activties

2011	Xue Zhao, Department of Physics, ETH Zürich, Semester thesis: "Characterization of polymeric cantilever arrays in different media"
2011	Xue Zhao, Department of Physics, ETH Zürich, Internship
2012	Xue Zhao, Department of Physics, ETH Zürich, Master Thesis: "Cantilever based sensing to quantify material-biosystem interactions"

Teaching Experience

2011	Teaching assistant: Biomaterials Science, Master program University of Bern

Generated Funding

Year	Source	Type	Project
2011-2012	SATW	Co-Applicant	TransferKolleg, Micro-Technologies for health applications, "Measuring contractile cell forces to identify nano- and microstructures for tailored medical implant surfaces"

Other Activities

2010	Top 10 finalists in IEEE Change the World competition (nLung: Novel nanoporous coatings to reduce harmful effects of toxic gases)

Membership in Professional Societies

Swiss Society for Biomaterials (2007 – present)
Swiss Society for Biomedical Engineering (2008 – present)
Biomedical Engineering Club, Bern (2009 - present, Founder member , President 2009 – present)
IEEE Engineering in Medicine & Biology society (2009 – present)
The Institution of Engineering and Technology (2009 – present)

Patent Applications

(PCT/EP2011/065325) "Injection molded micro cantilever and membrane sensor devices and process for their fabrication", Schift, Urwyler

Articles in Peer-Reviewed Journals

1. P. Urwyler, A. Pascual, P.M. Kristiansen, J. Gobrecht, B. Müller, H. Schift: *Mechanical and chemical stability of injection molded micro-cantilevers for sensing*, Journal of Applied Polymer Science **127** (2013) 2363-2370

2. J. Althaus, P. Urwyler, C. Padeste, R. Heuberger, H. Deyhle, H. Schift, J. Gobrecht, U. Pieles, D. Scharnweber, K. Peters and B. Müller: *Micro- and nanostructured polymer substrates for biomedical applications*, Proc. of SPIE **8339** (2012) 83390Q-83316

3. P. Urwyler, H. Deyhle, O. Bunk, P.M. Kristiansen, B. Müller: *Nanometersize anisotropy of injection molded polymer micro-cantilever arrays*, Journal of Applied Physics **111** (2012) 103530-103536

4. P. Urwyler, J. Köser, H. Schift, J. Gobrecht, B. Müller: *Nano-mechanical transduction of polymer micro-cantilevers to detect bio-molecular interactions*, Biointerphases **7** (2012) 6

5. P. Urwyler, H. Schift, J. Gobrecht, O. Häfeli, M. Altana, F. Battiston, B. Müller: *Surface patterned polymer micro-cantilever arrays for sensing*, Sensors and Actuators A : Physical **172** (2011) 2-8

6. P. Urwyler, O. Häfeli, H. Schift, J. Gobrecht, F. Battiston, B. Müller: *Disposable polymeric micro-cantilever arrays for sensing*, Procedia Engineering **5** (2010) 347-350

Peer-Reviewed Conference Abstracts

1. P. Urwyler, O. Häfeli, H. Schift, J. Gobrecht, B. Müller: *Disposable Polymeric Micro-Cantilever Arrays for Biomedical Applications*, European Cells and Materials **20** (2010) 48

2. P. Urwyler, O. Häfeli, H. Schift, J. Gobrecht, F. Battiston, B. Müller: *Polymeric micro-cantilever arrays for sensing*, European Cells and Materials **20** (2010) 261

3. P. Urwyler, J. Köser, H. Schift, J. Gobrecht, F. Battiston, B. Müller: *Injection-moulded micro-cantilever arrays for detecting DNA sequences*, European Cells and Materials **22** (2011) 29

References

- Prof. Dr. Bert Müller, Biomaterials Science Center, University of Basel, Switzerland
- Prof. Dr.-Ing. Jens Gobrecht, Laboratory for Micro- and Nanotechnology, Paul Scherrer Institut, Villigen, Switzerland
- Prof. Dr. Stephen Ferguson, Institute for Biomechanics, ETH Zurich, Switzerland
- Prof. Dr.-Ing. Lutz-P. Nolte, Director, Institute for Surgical Technology and Biomechanics, Medical Faculty, University of Bern, Switzerland

Aim/Objective

Seeking a challenging position in the biomedical engineering field utilizing my interdisciplinary expertise and experience.